Measurement of the Higgs boson cross sections and properties in the diphoton, ZZ and WW decay channels using the ATLAS detector

Marco Sessa

CERN, Università & INFN Roma Tre

SUSY2017 – Mumbai, 11-15 December 2017

Outline

- Higgs boson production at LHC

- ATLAS summary results:
  - $H \to ZZ^* \to 4\ell$
  - $H \to \gamma\gamma$
  - $H \to WW^* \to \ell\nu\ell\nu$

- Higgs properties measurement
  - Couplings
  - Width
  - Spin and parity

Higgs mass measurement not covered here
See dedicated talk by Marcello Fanti

- Summary and conclusions

All ATLAS Higgs results are available here:
https://twiki.cern.ch/twiki/bin/view/AtlasPublic/HiggsPublicResults

Main motivations for the Higgs searches

- The Higgs boson plays an important role in the SM: it provides mass to the elementary particles, through the electroweak spontaneous symmetry breaking (EWSB)

- It is a fantastic new tool to test the Standard Model of particle physics

- Several reasons to study the Higgs boson after its discovery:
  - Cross-section measurements
  - Couplings with SM particles
  - Improving of the precision on the Higgs mass
  - Higgs width
  - Spin-parity tests

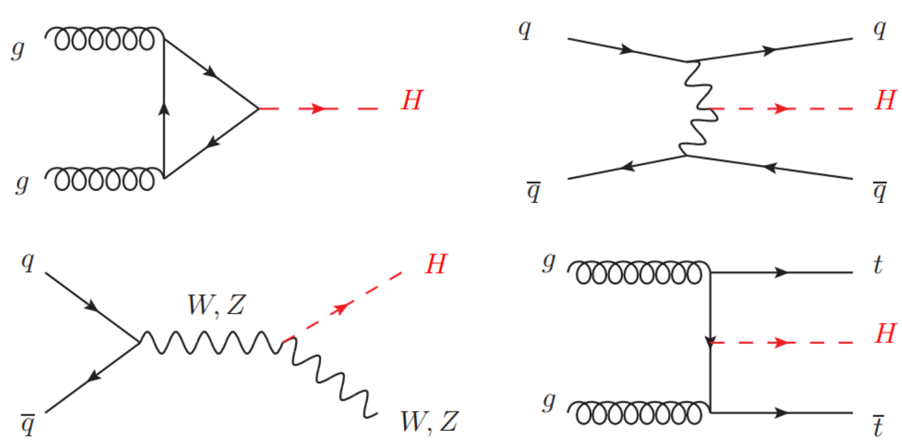

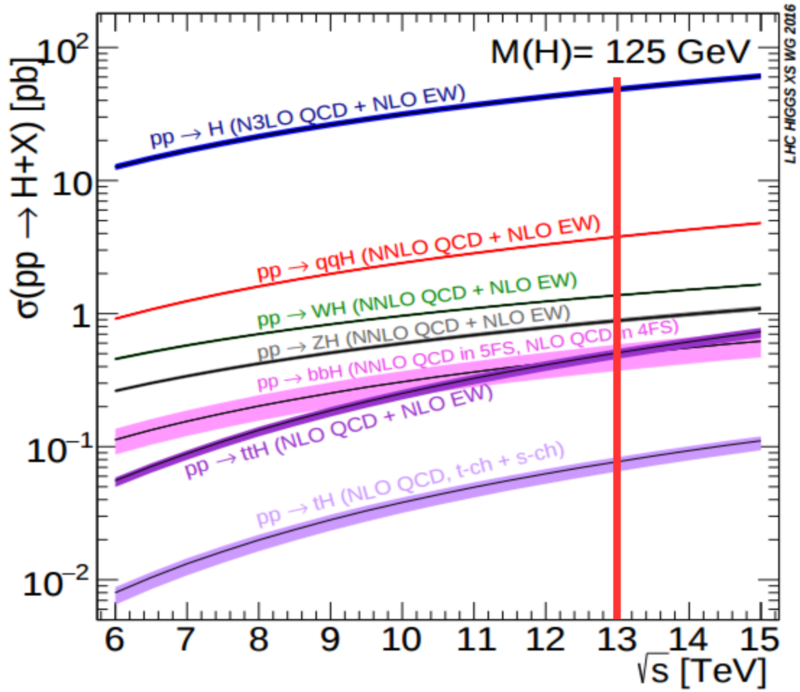

H→ZZ*→4ℓ

arXiv:1708.02810

- Low branching fraction: BR(H→ ZZ*) ~2.6%
  further reduced by [BR(Z→ee,μμ)]^2 = [6%]^2 ➡ BR(H→ZZ*→4l) ~ 0.01%

36.1 fb^{-1} @ 13 TeV

- High resolution on Higgs mass. Ratio S/B ~2 in the Higgs mass window (inclusive analysis)
- Non-resonant ZZ* background is the only relevant background in the analysis (irreducible background, estimated from MC simulations)
- Reducible backgrounds (Z+jets and top mainly) strongly suppressed with the event selection
- Fiducial cross-section extracted from events in the mass region 115 < m4ℓ < 130 GeV
- Measured inclusive fiducial cross-section: $3.62 \pm 0.50\ (\text{stat})\ {}^{+0.25}_{-0.20}\ (\text{sys})\ \text{fb}$
  in agreement with the SM prediction: $2.91 \pm 0.13\ \text{fb}$

$$\sigma_{i,\text{fid}} = \sigma_i \times A_i \times \mathcal{B} = \frac{N_{i,\text{fit}}}{\mathcal{L} \times C_i}, \quad C_i = \frac{N_{i,\text{reco}}}{N_{i,\text{part}}}$$

- Xsec*BR for the different production modes using a dedicated H→4ℓ candidate events categorization

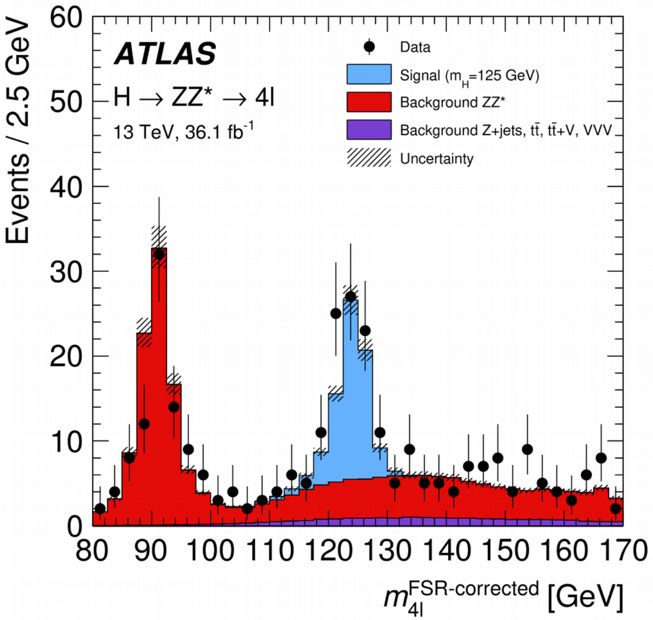

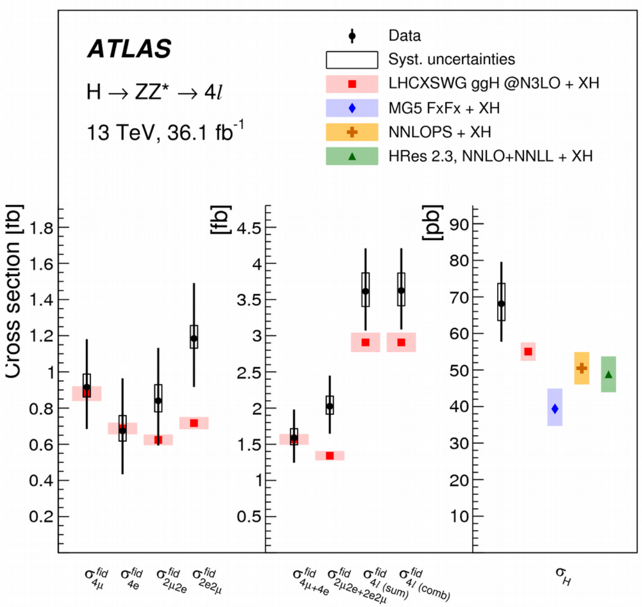

arXiv:1712.02304

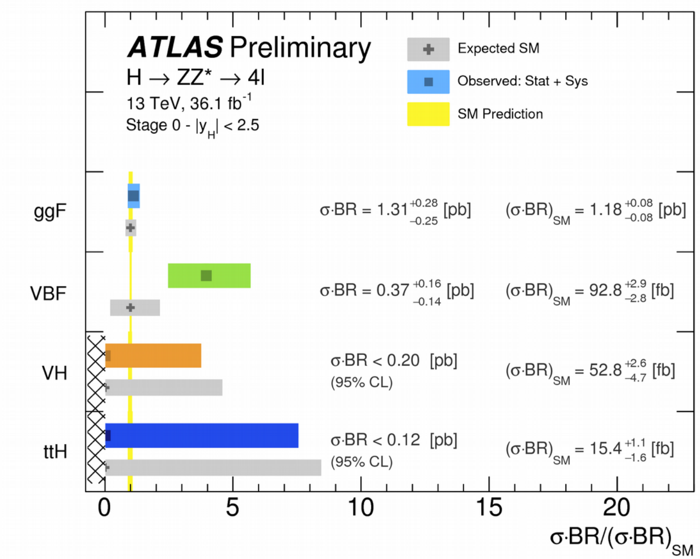

Fiducial differential distributions

arXiv:1708.02810

- Single and double differential cross-sections as a function of Higgs related variables Below single differential distributions: p_T ,rapidity (y) and Njets (exclusive and inclusive)
- Differential distributions sensitive to perturbative QCD calculations and presence of new additional particles in loops
- Good agreement with the SM expectations. Measurements still limited by statistical uncertainty

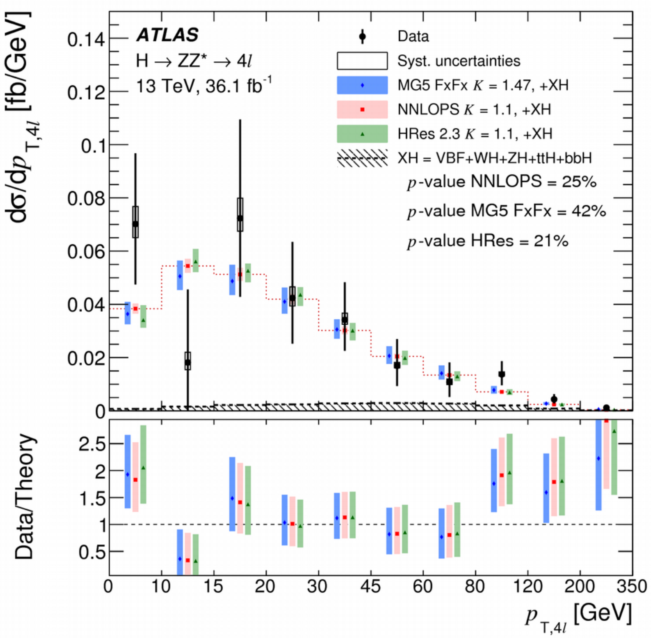

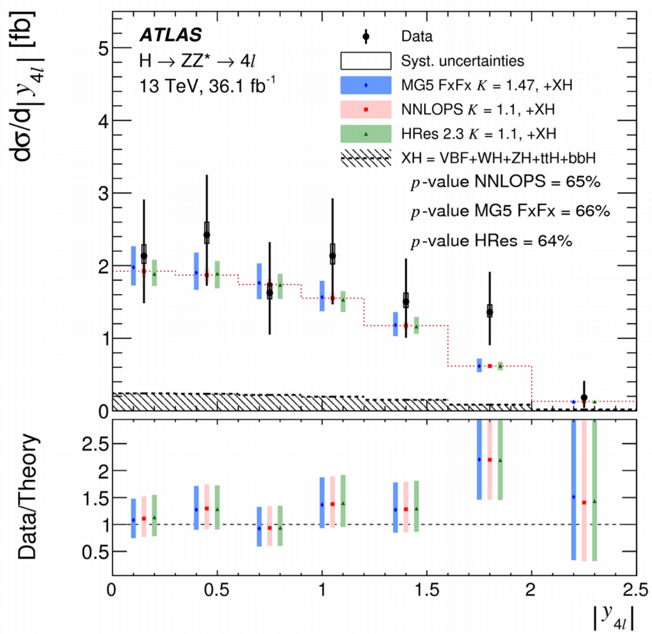

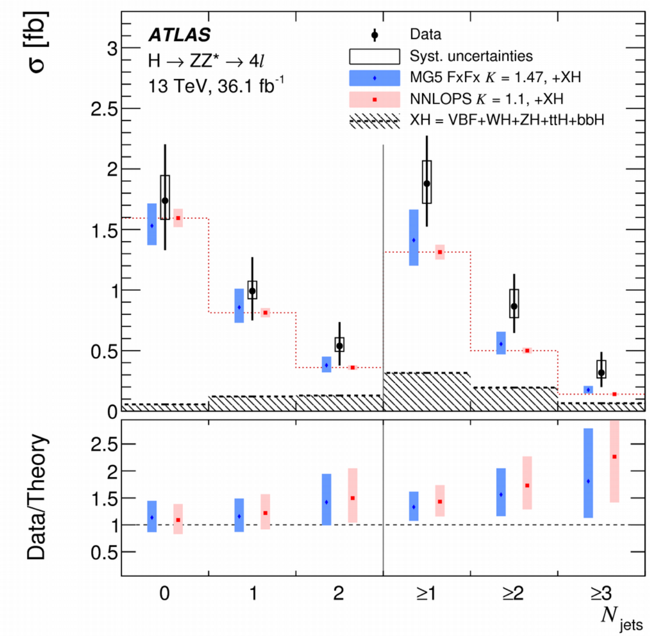

H→ZZ*→4ℓ - BSM searches

arXiv:1708.02810

- Differential cross section in the m12-m34 plane used to extract limits in the pseudo-observables framework
- Terms modifying the contact interaction between the Higgs and leptons or Z bosons

Eur. Phys. J. C **75** (2015) 128

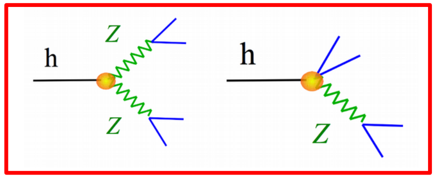

- Contact terms affect the invariant mass spectra and not the angular distributions
- Limits are extracted in the plane of:
  - ε_L and ε_R, which modify the contact terms between the Higgs boson and left-and right-handed leptons, assuming lepton-flavour universality
  - ε_L and κ, which modify the coupling of the Higgs boson to Z bosons
- The allowed observed area at the 95% CL is surrounded by the red solid line. This can be compared to the SM prediction, which is indicated by the black star and the black dotted line

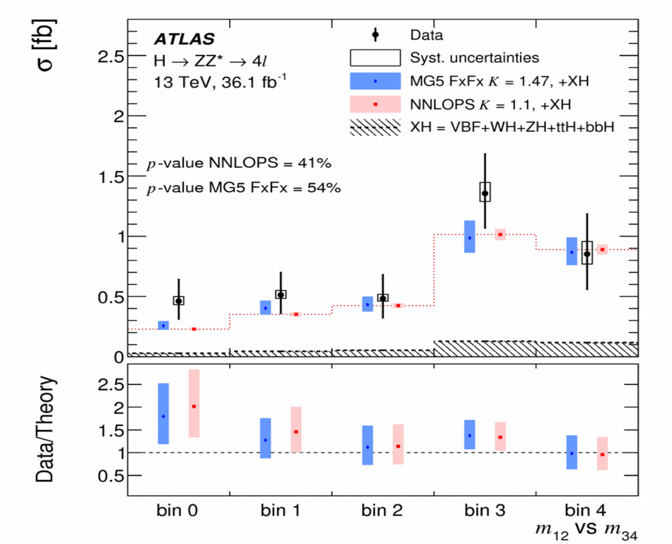

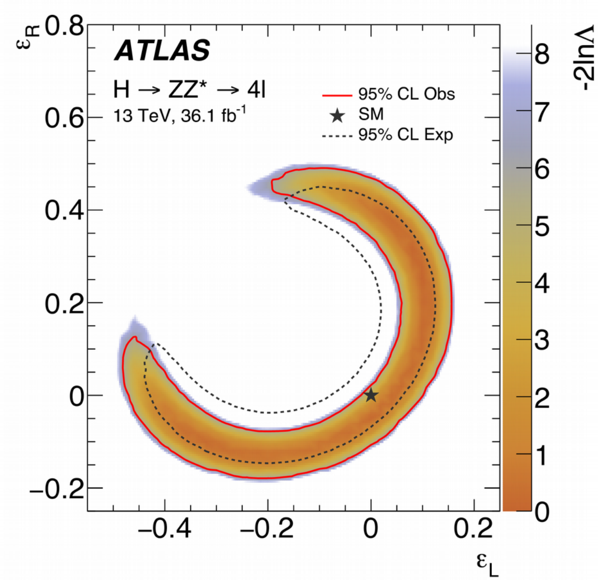

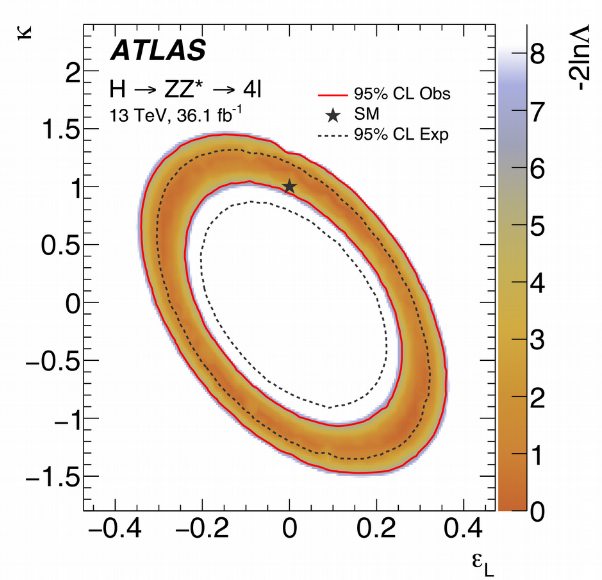

- <u>No deviations from the SM are observed</u>

H→γγ

ATLAS-CONF-2017-045

36.1 fb^{-1} @ 13 TeV

BR(H->γγ) ~ 0.23%

- Clean experimental signature and good invariant mass resolution
- Analysis performed exploiting an event categorization to target the main Higgs production modes
- Signal yield extracted from a simultaneous signal+background fit of the $m_{\gamma\gamma}$ distribution
- Background function chosen as the one that minimizes the fitted signal yield in signal+background fits in a background control sample. Double-sided Crystal Ball function for the signal modeling
- Signal strength: $\mu = 0.99\ ^{+0.12}_{-0.11}\ (\text{stat.})\ ^{+0.06}_{-0.05}\ (\text{exp.})\ ^{+0.06}_{-0.05}\ (\text{theory})$

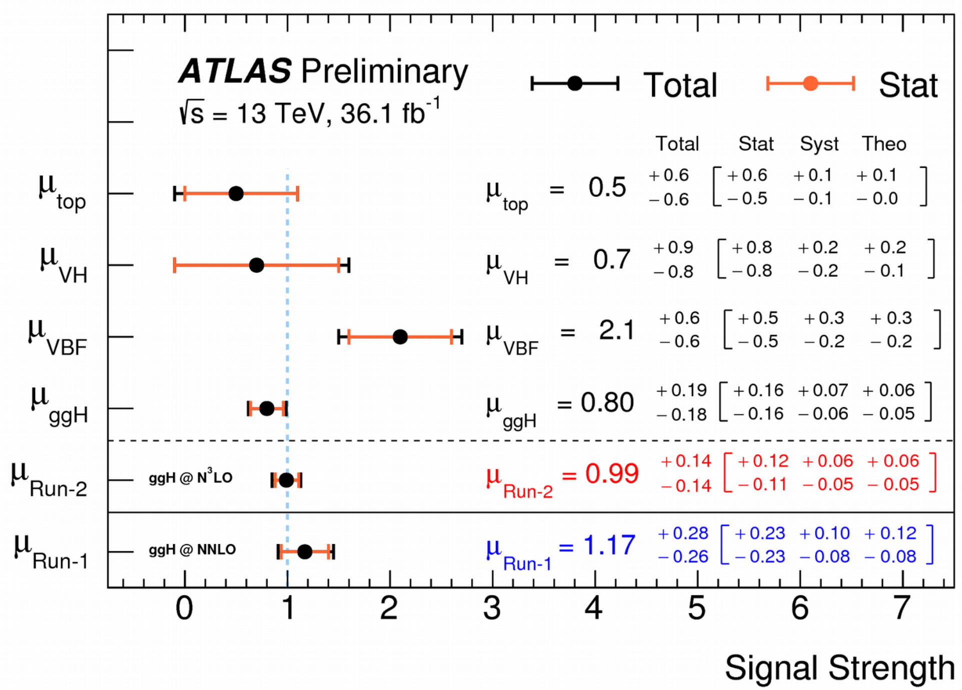

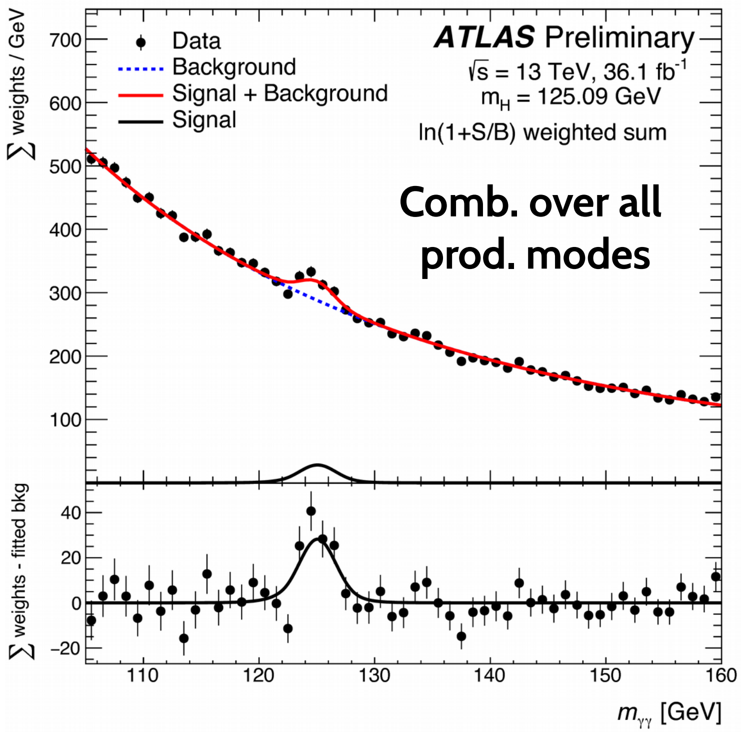

- Single differential cross-sections as a function of Higgs related variables: p_T, rapidity (y)
- The measurements are compared to several state-of-the-art predictions of gluon fusion

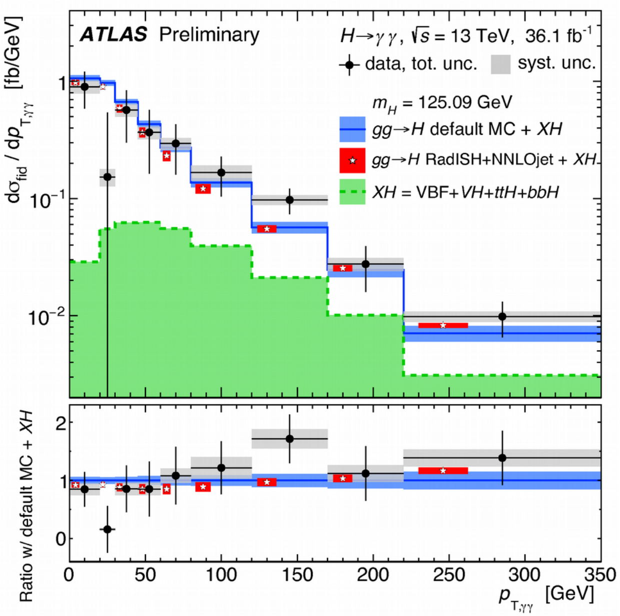

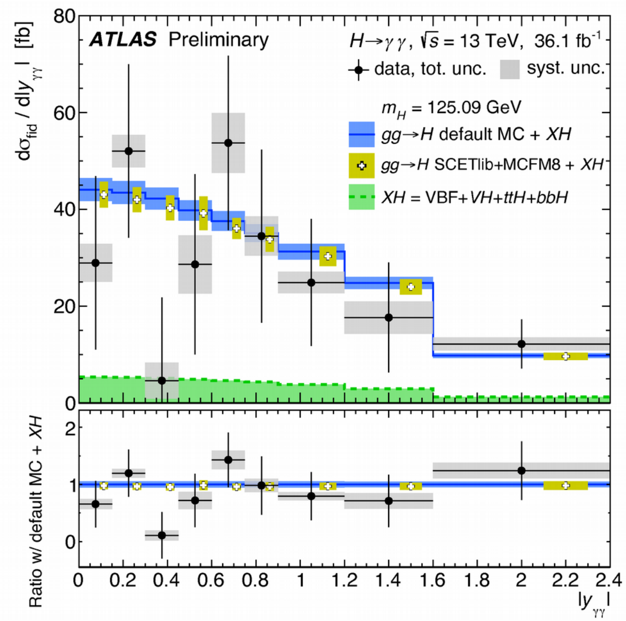

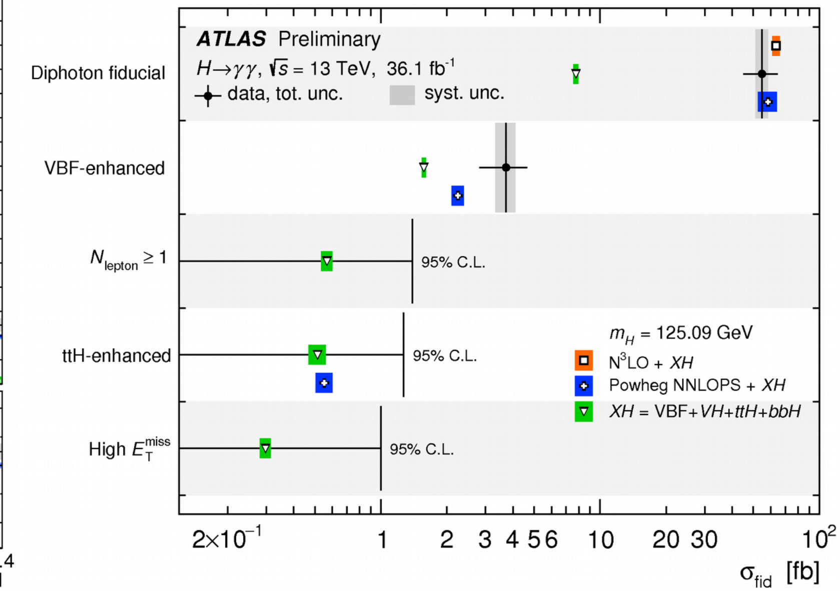

- Cross sections in several fiducial regions are measured: these regions target either specific Higgs boson production mechanisms or are sensitive to the presence of physics beyond the Standard Model.

- Inclusive fiducial cross-section: σ_{fid} = 54.7 ± 9.1 (stat.) ± 4.5 (syst.) fb
- The Standard Model prediction for the same fiducial region is 63.5 ± 2.4 fb

H→ZZ*→4ℓ and H→γγ combination

ATLAS-CONF-2017-047

36.1 fb^{-1} @ 13 TeV

- Full combination @ 13 TeV of H→ZZ*→4ℓ and H→γγ searches
- Global signal strength: $\mu = 1.09 \pm 0.09\ (\text{stat.})\ ^{+0.06}_{-0.05}\ (\text{exp.})\ ^{+0.06}_{-0.05}\ (\text{th.})$

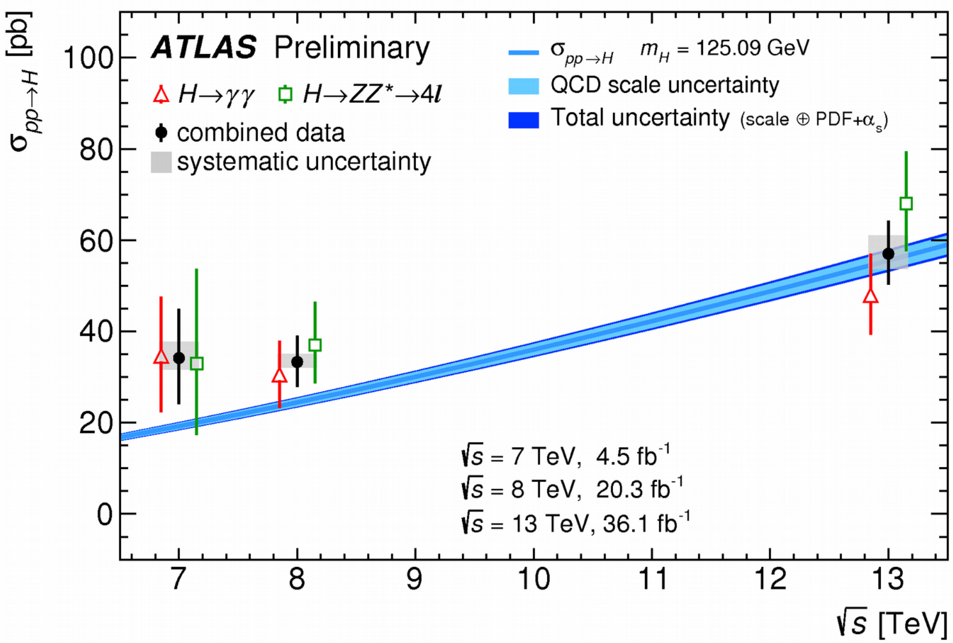

Measurement at 13 TeV

$57.0^{+6.0}_{-5.9}\ (\text{stat.})\ ^{+4.0}_{-3.3}\ (\text{syst.})$ pb

SM prediction

$55.6^{+2.4}_{-3.4}$ pb

Total pp → H+X cross sections measured at different centre-of-mass energies compared to Standard Model predictions at up to N3LO in QCD

Excellent agreement with the SM predictions
Accuracy dominated by statistical uncertainty

Decay channel	Total cross section ($pp \to H + X$)		
	$\sqrt{s}$ =7 TeV	$\sqrt{s}$ =8 TeV	$\sqrt{s}$ =13 TeV
$H \to \gamma\gamma$	35^{+13}_{-12} pb	$30.5^{+7.5}_{-7.4}$ pb	$47.9^{+9.1}_{-8.6}$ pb
$H \to ZZ^* \to 4\ell$	33^{+21}_{-16} pb	37^{+9}_{-8} pb	$68.0^{+11.4}_{-10.4}$ pb
Combination	$34 \pm 10\ (\text{stat.})\ ^{+4}_{-2}\ (\text{syst.})$ pb	$33.3^{+5.5}_{-5.3}\ (\text{stat.})\ ^{+1.7}_{-1.3}\ (\text{syst.})$ pb	$57.0^{+6.0}_{-5.9}\ (\text{stat.})\ ^{+4.0}_{-3.3}\ (\text{syst.})$ pb
SM prediction [8]	19.2 ± 0.9 pb	24.5 ± 1.1 pb	$55.6^{+2.4}_{-3.4}$ pb

H→ZZ*→4ℓ and H→γγ combination

ATLAS-CONF-2017-047

- Higgs boson cross-section for different production modes
  - bbH included in ggF, tH included in ttH
  - assuming SM Higgs decay branching fractions

- Largest deviation in VBF
  - 2.2 sigma above the expectation in both H→ZZ*→4ℓ and H→γγ

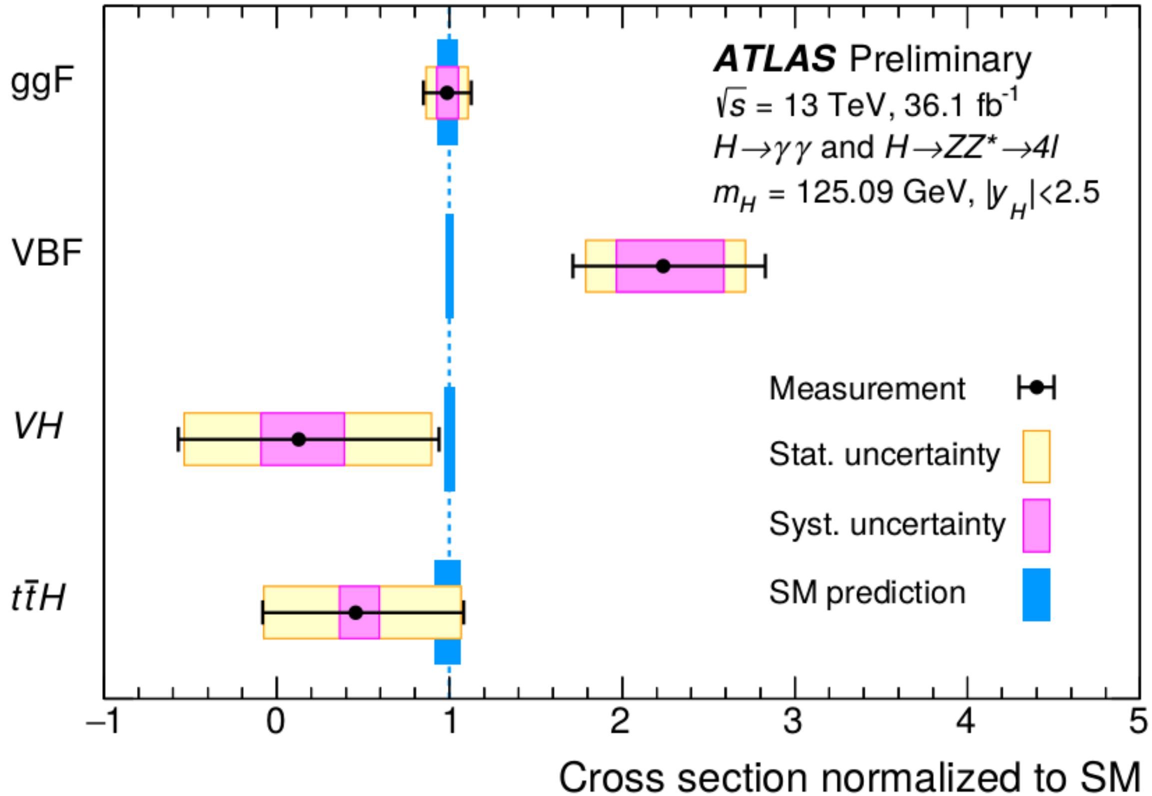

Higgs couplings

- The cross section results by production mode (Stage 0 of STXS, see back-up) can also be interpreted within the κ framework with coupling modifiers κ_V and κ_F, to probe separately the Higgs couplings with the SM bosons and fermions
- $H \to ZZ^* \to 4\ell$ and $H \to \gamma\gamma$ combination @ 13 TeV
- SM predictions consistent with the measurements, within the experimental uncertainties

ATLAS-CONF-2017-047

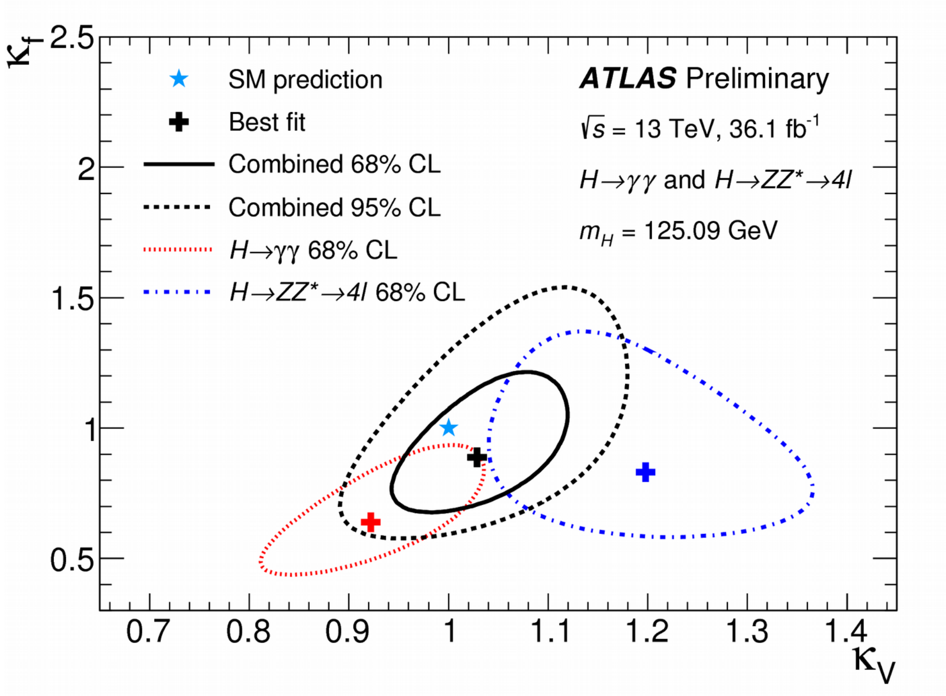

$H \rightarrow WW^* \rightarrow \ell\nu\ell\nu$

5.8 fb^{-1} @ 13 TeV

- 2nd largest Higgs branching fraction → BR($H \rightarrow WW^*$) ~ 22%
- Access for measurement of the Higgs boson couplings with vectors bosons (W and Z) and fermions (top mainly)
- Analysis restricted to two distinctive production modes (VBF and WH)
- Background normalizations estimated from data using CR: CRs and SRs fit together to extract the NFs and signal strength

- **VBF: eμ + 2 jets**
- **Different lepton flavours to reject Drell-Yan**
- **BDT used to select VBF Higgs topology**

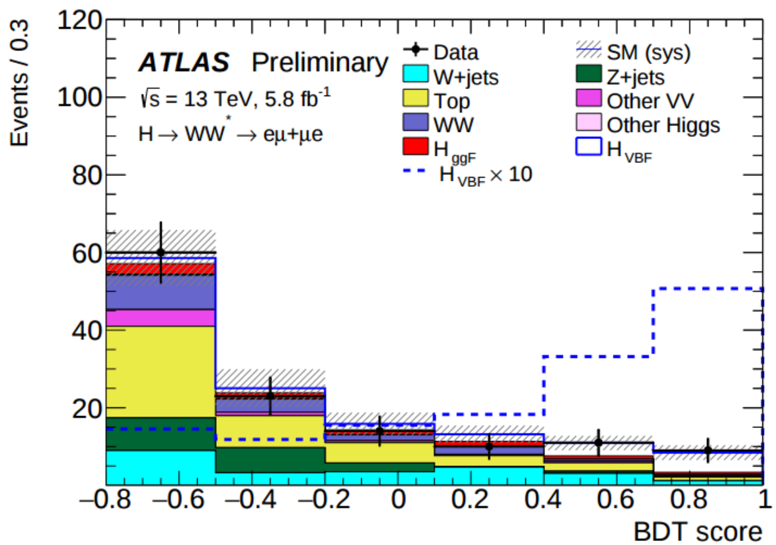

$$\mu_{\text{VBF}} = 1.7^{+1.0}_{-0.8}(\text{stat})^{+0.6}_{-0.4}(\text{sys})$$

Observed (expected) significance: 1.9σ (1.2σ)

- **WH: 3ℓ events**
- **High MET, ≤ 1 jets**
- **two SR categories, split according to the presence of same flavor OS leptons**

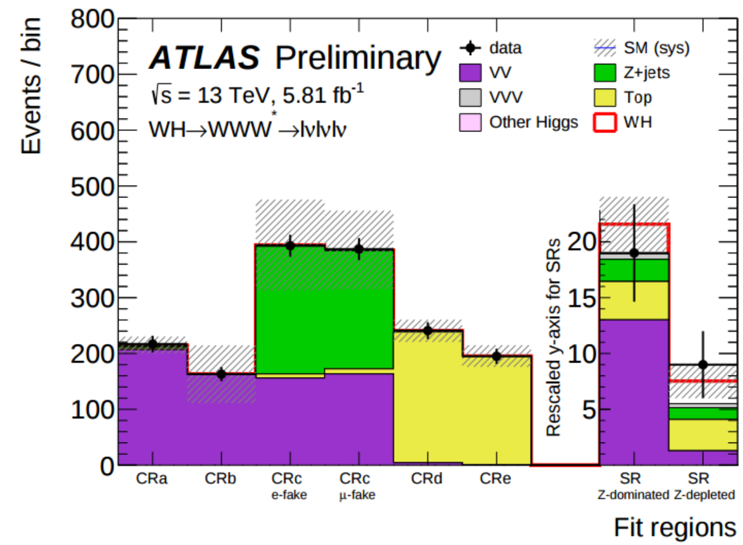

$$\mu_{WH} = 3.2^{+3.7}_{-3.2}(\text{stat})^{+2.3}_{-2.7}(\text{sys})$$

Observed (expected) significance: 0.77σ (0.24σ)

Eur. Phys. J. C (2015) 75:335

Higgs width

~20.3 fb^{-1} @ 8 TeV

- SM prediction for a Higgs boson with m_H = 125 GeV → Γ_h = 4.07 MeV
- A deviation would imply a decay to non-SM particles
- Γ_h cannot be accessed directly (experimental resolution ~1-2 GeV)
- In the Higgs off-shell regime, $\sigma_{off\text{-}shell}$ does not depend on the total width Γ_H, while $\sigma_{on\text{-}shell}$ does
- Under the assumption of equal on-peak and off-peak coupling modifiers, limit on μ off-shell can be reinterpreted as limit on Γ_H

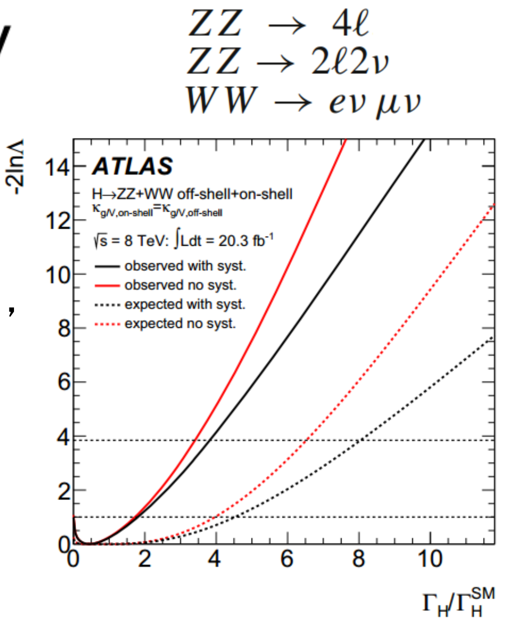

Γ_H < 22.7 MeV @ 95%CL
(<33 MeV exp.)

Eur. Phys. J. C75 (2015) 476

Higgs spin-parity

~25 fb^{-1} @ 7-8 TeV

- Run 1 analysis performed exploiting Higgs boson decaying in WW^*, ZZ^* and γγ boson pairs
- SM predicts the Higgs boson quantum numbers to be $J^{PC}=0^{++}$ (H→γγ decay forbids Higgs to be J=1)
- This reflects in the angular distributions of the final decay products
- Construct statistic to test hypothesis "X" vs SM spin-CP hypothesis. Many alternative hypothesis tested (0^-, BSM 0^+ and 2^+)
- The combination of the three decays processes allows to exclude all the considered non-SM spin hypothesis at more than 99.9% CL in favour of the SM spin-0 hypothesis

Conclusions and prospects

- Overview of the ATLAS analyses with Higgs boson decaying in vectors bosons using Run 1 and Run 2 data
- Results shown in terms of (fiducial) integrated and differential cross-sections, couplings and Higgs boson properties (width, spin-parity)
- All the results are consistent with the SM predictions
- Most of the measurements are limited by statistics, but…

- …plenty of data ready to be analyzed!
  - New ~45 fb^{-1} recorded during 2017 data-taking
  - Entering a new era of Higgs precision measurements

Back-up slides

Higgs cross-sections at 13 TeV

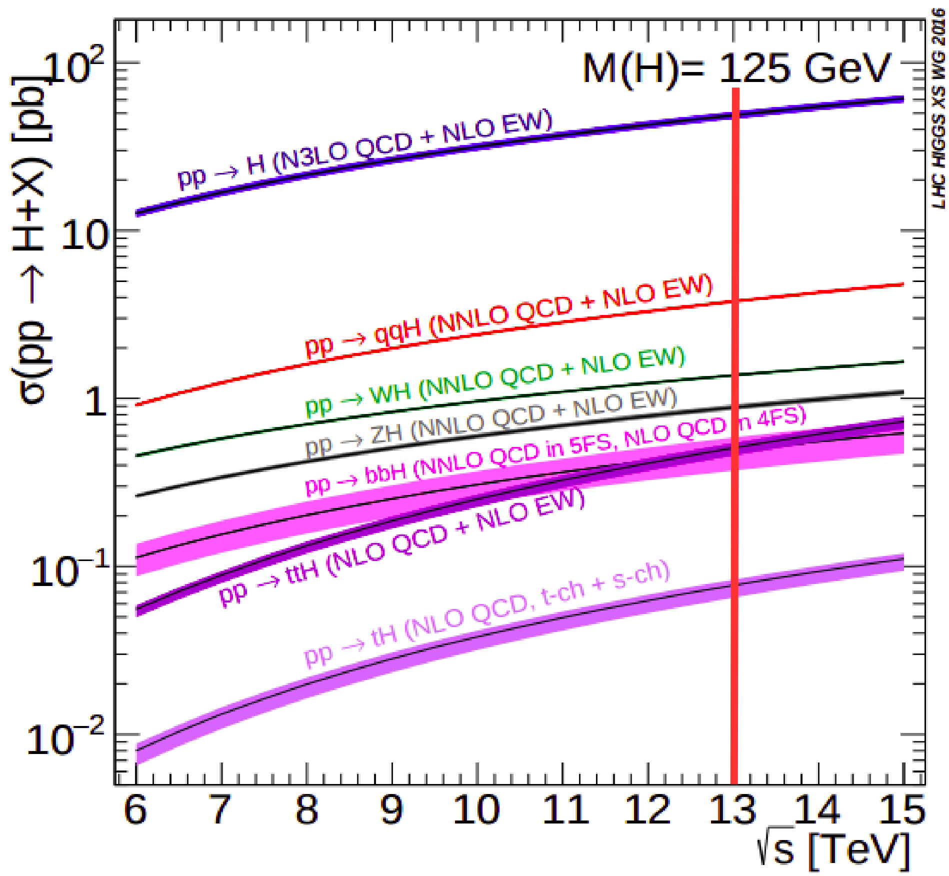

Process	Cross section [pb]	Calculation
ggF	$43.92^{+7.4\%}_{-7.9\%}(\text{QCD Scale})^{+7.1\%}_{-6.0\%}(\text{PDF} + \alpha_S)$	NNLO+NNLL QCD, NLO EW
VBF	$3.748^{+0.7\%}_{-0.7\%}(\text{QCD Scale})^{+3.2\%}_{-3.2\%}(\text{PDF} + \alpha_S)$	NNLO QCD, NLO EW
WH	$1.380^{+0.7\%}_{-1.5\%}(\text{QCD Scale})^{+2.2\%}_{-2.2\%}(\text{PDF} + \alpha_S)$	NNLO QCD, NLO EW
ZH	$0.8696^{+3.8\%}_{-3.8\%}(\text{QCD Scale})^{+2.2\%}_{-2.2\%}(\text{PDF} + \alpha_S)$	NNLO+NNLL QCD, NLO EW
ttH	$0.5085^{+5.7\%}_{-9.3\%}(\text{QCD Scale})^{+8.8\%}_{-8.8\%}(\text{PDF} + \alpha_S)$	NNLO QCD

Higgs branching fractions

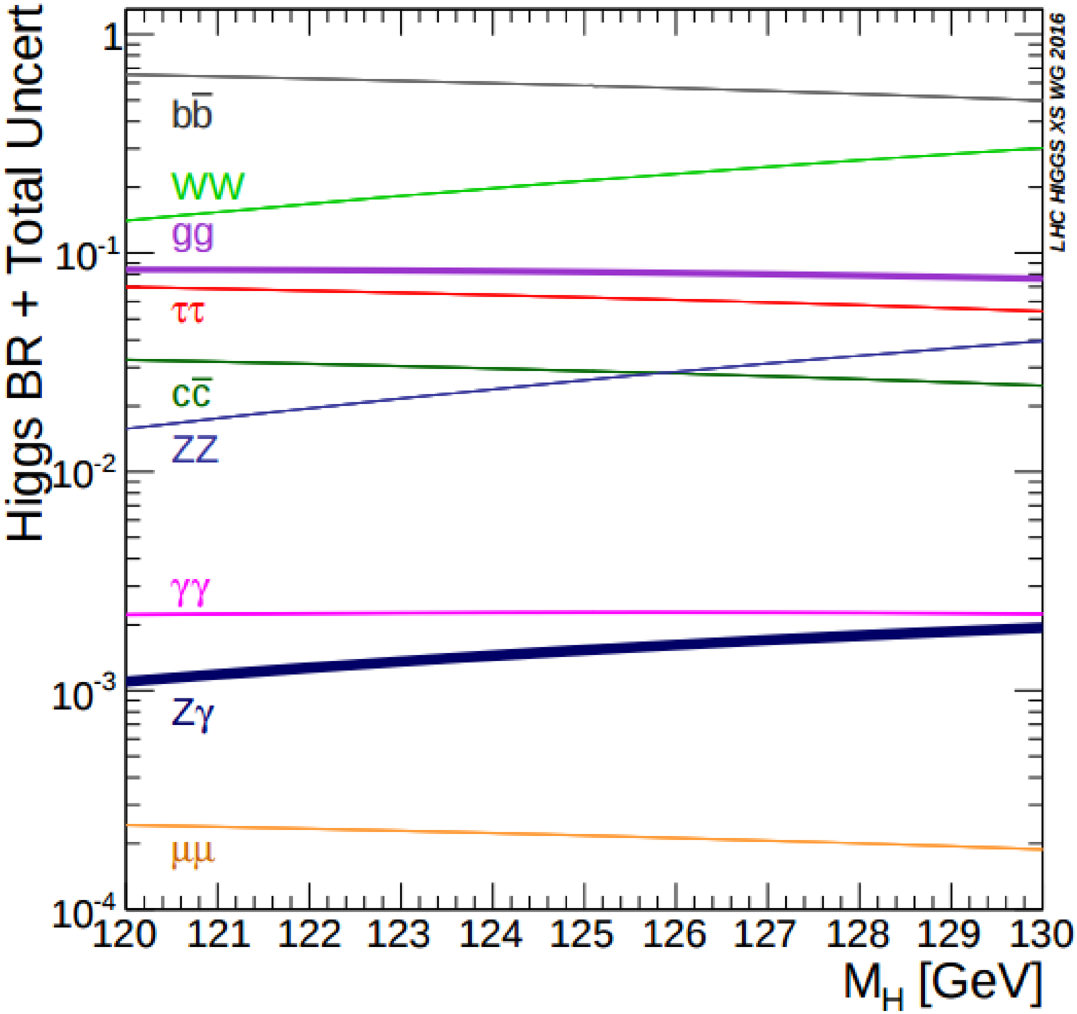

Decay mode	Branching fraction [%]
$H \to bb$	57.5 ± 1.9
$H \to WW$	21.6 ± 0.9
$H \to gg$	8.56 ± 0.86
$H \to \tau\tau$	6.30 ± 0.36
$H \to cc$	2.90 ± 0.35
$H \to ZZ$	2.67 ± 0.11
$H \to \gamma\gamma$	0.228 ± 0.011
$H \to Z\gamma$	0.155 ± 0.014
$H \to \mu\mu$	0.022 ± 0.001

$H \to ZZ^* \to 4\ell$

arXiv:1708.02810

Selections used for the fiducial space definition

Leptons and jets	
Muons:	$p_T > 5$ GeV, $\|\eta\| < 2.7$
Electrons:	$p_T > 7$ GeV, $\|\eta\| < 2.47$
Jets:	$p_T > 30$ GeV, $\|y\| < 4.4$
Jet–lepton overlap removal:	$\Delta R(\text{jet}, \ell) > 0.1$ (0.2) for muons (electrons)
Lepton selection and pairing	
Lepton kinematics:	$p_T > 20, 15, 10$ GeV
Leading pair (m_{12}):	SFOS lepton pair with smallest $\|m_Z - m_{\ell\ell}\|$
Subleading pair (m_{34}):	remaining SFOS lepton pair with smallest $\|m_Z - m_{\ell\ell}\|$
Event selection (at most one quadruplet per channel)	
Mass requirements:	50 GeV$< m_{12} <$ 106 GeV and 12 GeV$< m_{34} <$ 115 GeV
Lepton separation:	$\Delta R(\ell_i, \ell_j) > 0.1$ (0.2) for same- (different-)flavour leptons
J/ψ veto:	$m(\ell_i, \ell_j) > 5$ GeV for all SFOS lepton pairs
Mass window:	115 GeV$< m_{4\ell} <$ 130 GeV

$H \rightarrow ZZ^* \rightarrow 4\ell$, classification of the Higgs boson production modes (STXS)

- STXS were designed to measure the different Higgs production processes in specific regions of phase space and in a way that can be easily combined with other decay channels. Compared to the signal strength measurements, they provide a finer granularity, and thus more information for theoretical interpretations. A second advantage of such approach is that the theory uncertainties folded ilto the results are smaller, since the cross sections are defined in simplified, mutually exclusive fiducial volumes without any model-dependent extrapolation to the total phase space
- Production cross section times BR is measured in mutually exclusive phase space regions (production bins), with $|y_H| < 2.5$
- Chosen to maximise the measurement precision and the sensitivity to BSM contributions

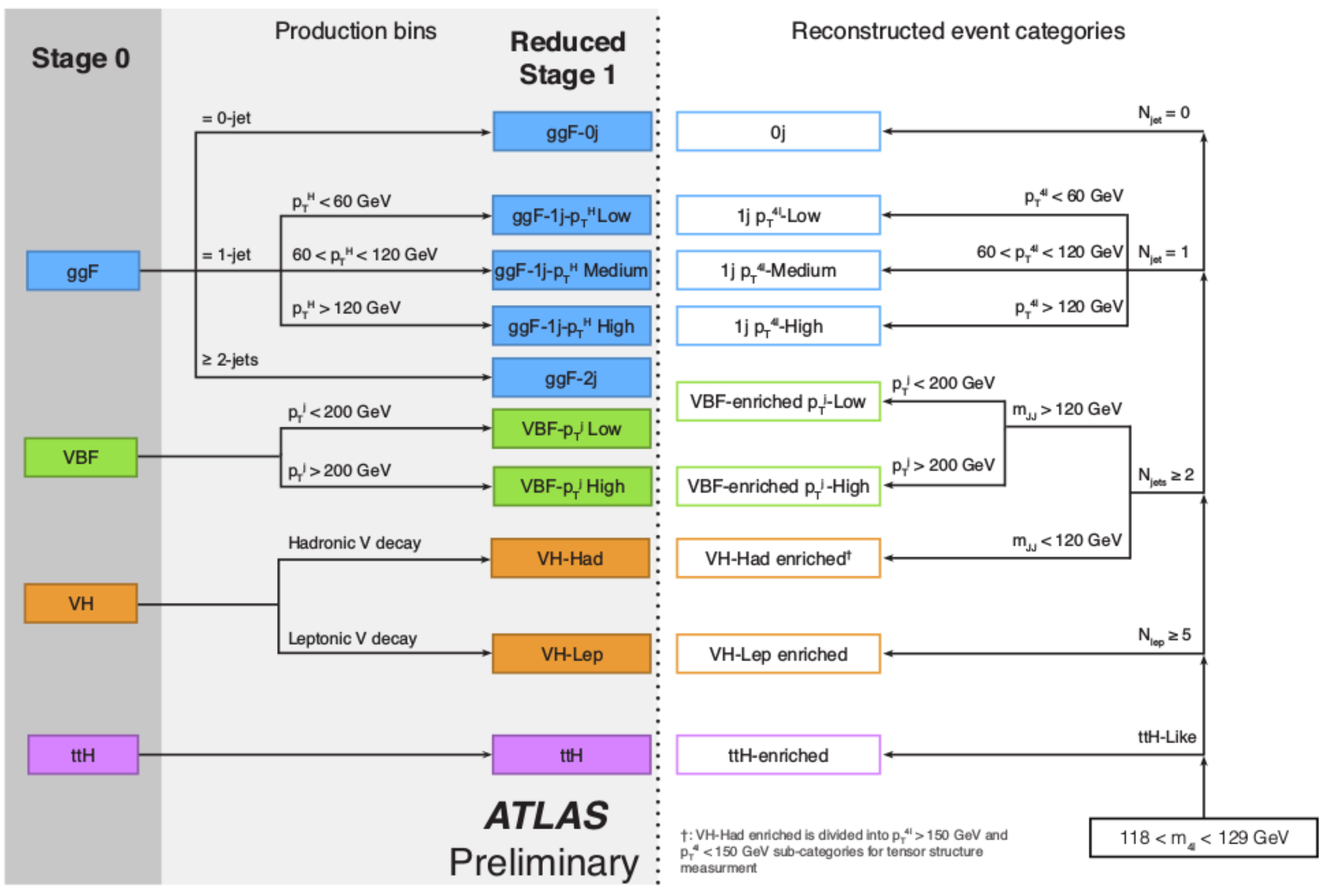

H→ZZ*→4ℓ, classification of the Higgs boson production modes (STXS)

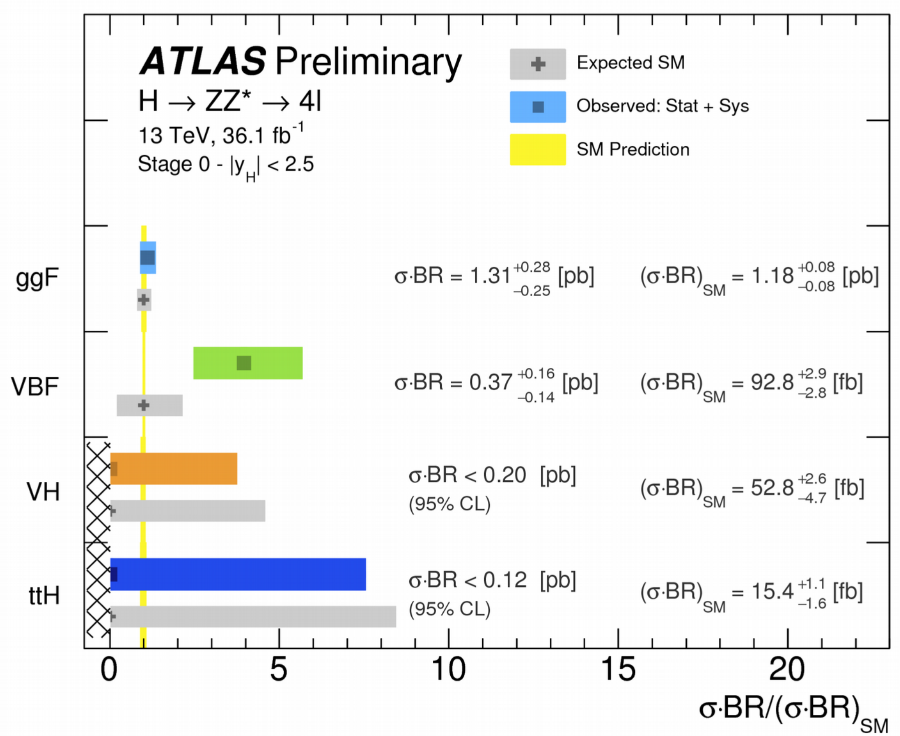

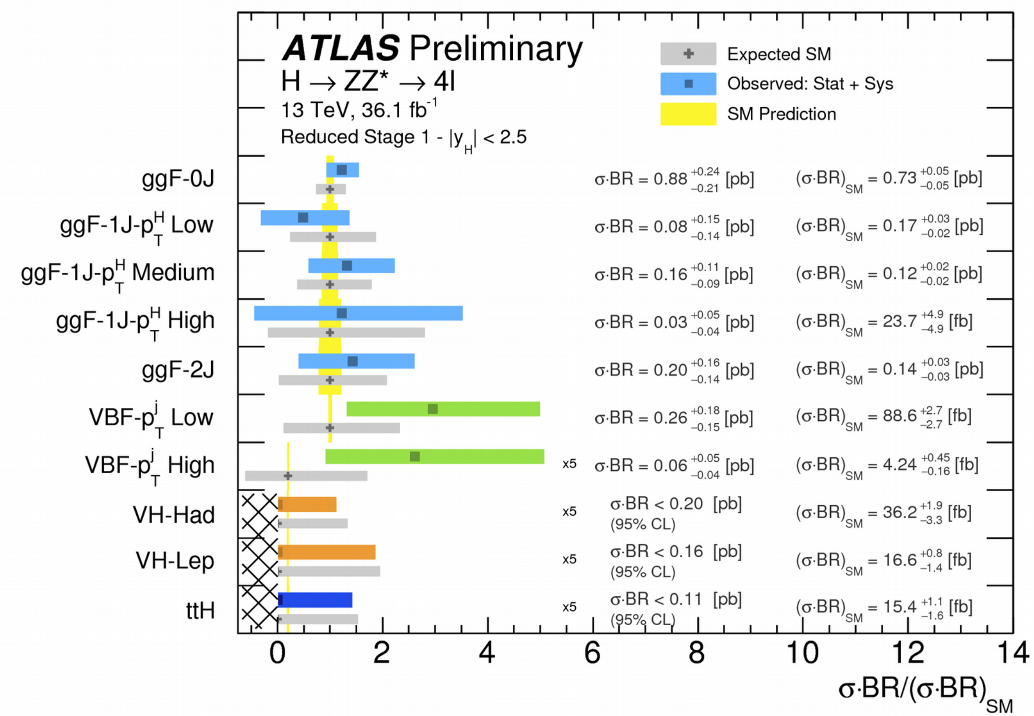

H→ZZ*→4ℓ - Fiducial differential distributions

arXiv:1708.02810

- Single and double differential cross-sections as a function of Higgs related variables: p_T, rapidity (y), cosθ* (top row), p_T & Njets = 0, 1 and ≥ 2 (bottom row)
- Differential distributions sensitive to perturbative QCD calculations and presence of new additional particles in loops

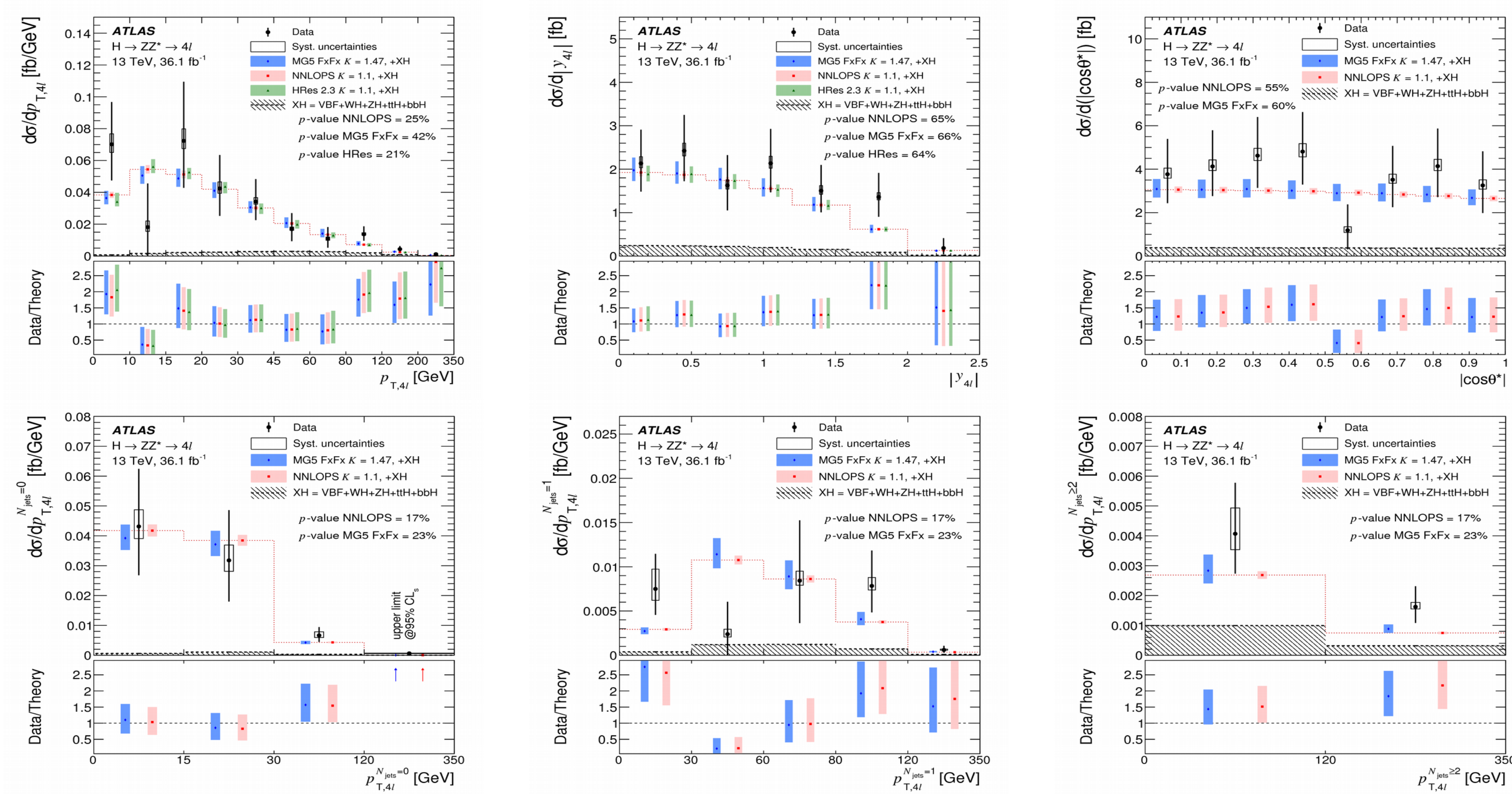

H→ZZ*→4ℓ - Fiducial differential distributions

arXiv:1708.02810

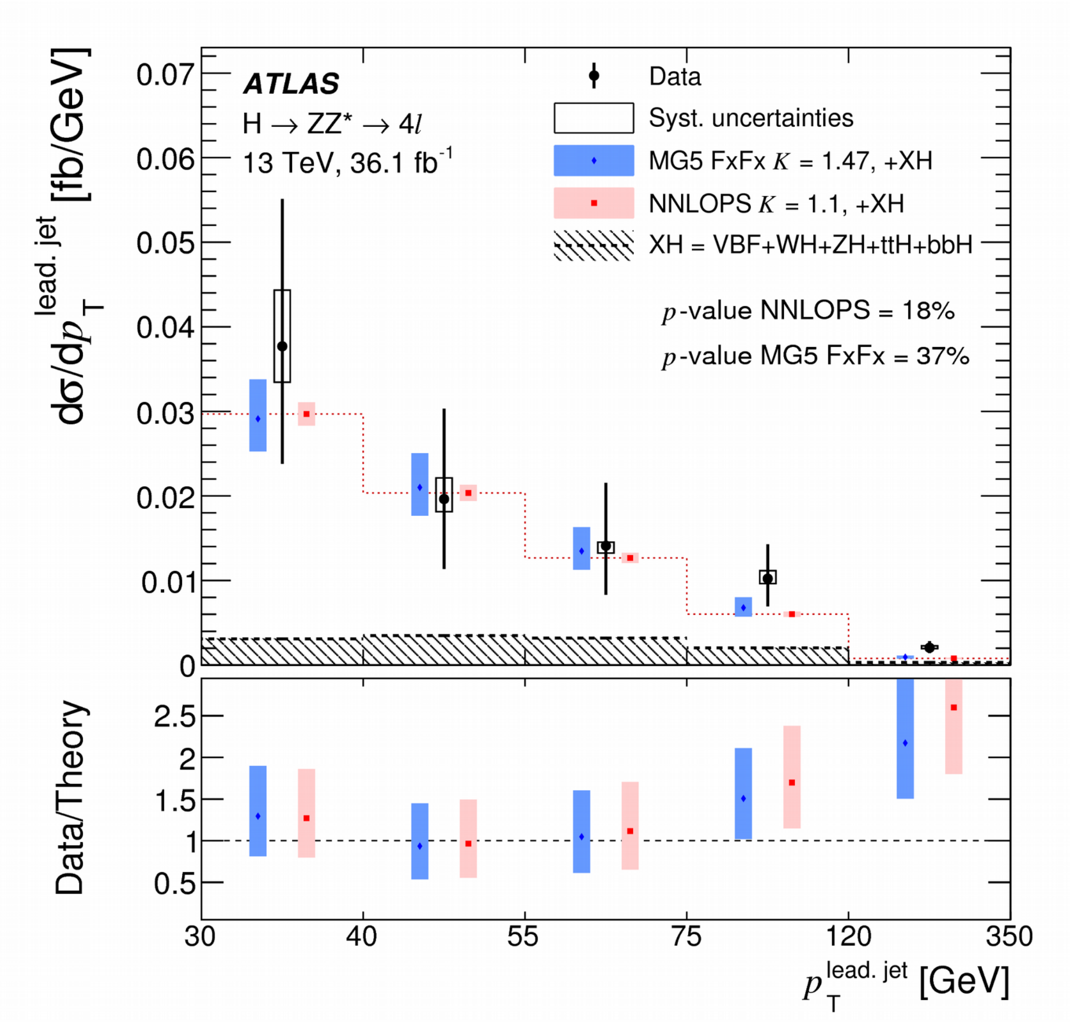

H→ZZ*→4ℓ – MC generators

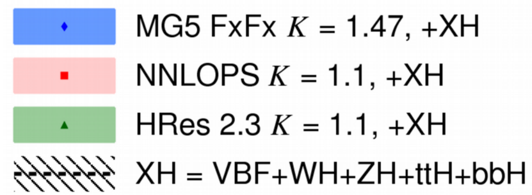

The Powheg-Box v2 Monte Carlo (MC) event generator [52–54] is used to simulate ggF [55], VBF [56] and VH [57] processes, using the PDF4LHC NLO PDF set [58]. The ggF Higgs boson production is accurate to NNLO in QCD, using the Powheg method for merging the NLO Higgs boson plus jet cross section with the parton shower, and the MiNLO method [59, 60] to simultaneously achieve NLO accuracy for inclusive Higgs boson production. Furthermore, a reweighting procedure is performed using the HNNLO program [61–63] to achieve full NNLO accuracy [64]. This sample is referred to as NNLOPS. The VBF and VH samples are produced at NLO accuracy in QCD. For VH, the MiNLO method is used to merge zero- and one-jet events. For Higgs boson production in association with a heavy quark pair, events are simulated at NLO with MadGraph5_aMC@NLO (v.2.2.3 for $t\bar{t}H$ and v.2.3.3 for $b\bar{b}H$) [65], using the CT10nlo PDF set [66] for $t\bar{t}H$ and the NNPDF23 PDF set [67] for $b\bar{b}H$. For the ggF, VBF, VH, and $b\bar{b}H$ production mechanisms, Pythia 8 [68, 69] is used for the $H \to ZZ^* \to 4\ell$ decay as well as for parton showering, hadronization, and multiple partonic interactions using the AZNLO parameter set [70]. For the $t\bar{t}H$ production mechanism, Herwig++ [71, 72] is used with the UEEE5 parameter set [73].
An alternative prediction for ggF SM Higgs boson production is generated using MadGraph5_aMC@NLO v.2.3.3 at NLO accuracy in QCD for zero, one, two additional jets, merged with the FxFx scheme [65, 74], using the NNPDF30_nlo_as_0118 PDF set [75]. This MG5_aMC@NLO_FxFx sample is interfaced to Pythia 8 for Higgs boson decay, parton showering, hadronization and multiple partonic interactions using the A14 parameter set [76]. The data are also compared to ggF SM Higgs boson production in the 4ℓ decay channel simulated with HRes v2.3 [63, 77], using the MSTW2008 NNLO PDF set [78]. The HRes program computes fixed-order cross sections for ggF SM Higgs boson production up to NNLO in QCD and describes the $p_{T,4\ell}$ distribution at NLO. All-order resummation of soft-gluon effects at small transverse momenta is consistently included up to next-to-next-to-leading logarithmic order (NNLL) in QCD, using dynamic factorization and resummation scales (the central scales are chosen to be $m_H/2$). The program implements top quark and bottom quark mass dependence up to next-to-leading logarithmic order (NNL) + NLO in QCD. At NNLL + NNLO accuracy only the top quark contribution is considered. HRes does not perform parton showering and QED final-state radiation effects are not included. Both the MG5_aMC@NLO_FxFx and the HRes predictions are normalized using the LHCXSWG cross section.

H→ZZ*→4ℓ – BSM searches

arXiv:1708.02810

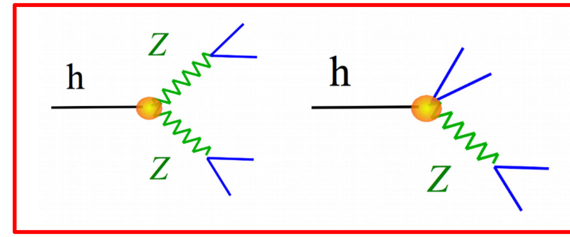

The m12 vs m34 kinematic plane is divided into five regions and projected onto a one-dimensional distribution

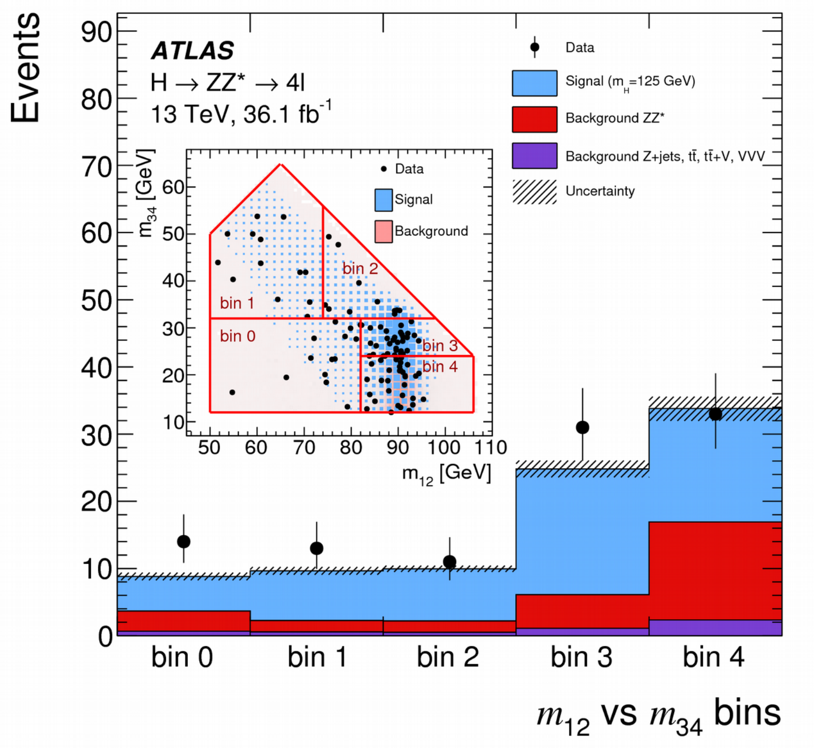

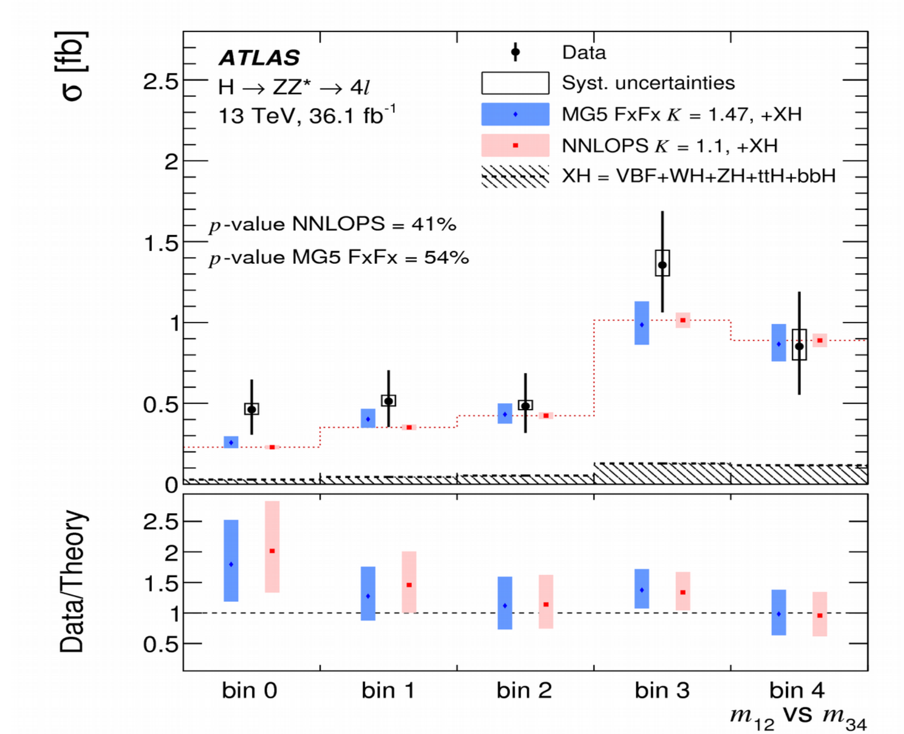

Since the contact terms have the same Lorentz structure as the SM term, they only affect the dilepton invariant mass spectra, while the lepton angular distributions are not modified. The difference in χ^2 between the measured and predicted cross sections in the m_{12} vs m_{34} parameter plane is therefore used to constrain the possible contributions from contact interactions.

H→γγ

Syst. uncertainties on the signal strength

Uncertainty Group	$\sigma_{\mu}^{\text{syst.}}$
Theory (yield)	0.03
Experimental (yield)	0.02
Luminosity	0.03
Theory (migrations)	0.05
Experimental (migrations)	0.01
Mass resolution	0.03
Mass scale	0.04
Background shape	0.03

$$\mu_{\text{ggH}} = 0.80\,^{+0.19}_{-0.18} = 0.80\,^{+0.16}_{-0.16}\,(\text{stat.})\,^{+0.07}_{-0.06}\,(\text{exp.})\,^{+0.06}_{-0.05}\,(\text{theory})$$

$$\mu_{\text{VBF}} = 2.1\,^{+0.6}_{-0.6} = 2.1\,^{+0.5}_{-0.5}\,(\text{stat.})\,^{+0.3}_{-0.2}\,(\text{exp.})\,^{+0.3}_{-0.2}\,(\text{theory})$$

$$\mu_{\text{VH}} = 0.7\,^{+0.9}_{-0.8} = 0.7\,^{+0.8}_{-0.8}\,(\text{stat.})\,^{+0.2}_{-0.2}\,(\text{exp.})\,^{+0.2}_{-0.1}\,(\text{theory})$$

$$\mu_{\text{top}} = 0.5\,^{+0.6}_{-0.6} = 0.5\,^{+0.6}_{-0.5}\,(\text{stat.})\,^{+0.1}_{-0.1}\,(\text{exp.})\,^{+0.1}_{-0.0}\,(\text{theory})$$

$$\mu = 0.99\,^{+0.14}_{-0.14} = 0.99\,^{+0.12}_{-0.11}\,(\text{stat.})\,^{+0.06}_{-0.05}\,(\text{exp.})\,^{+0.06}_{-0.05}\,(\text{theory})$$

Run-1 result: $\mu = 1.17 \pm 0.27$

Measured cross-sections

$$\sigma_{\text{ggH}} \times B(H \to \gamma\gamma) = 82\,^{+18}_{-18}\text{ fb} = 82^{+16}_{-16}\,(\text{stat.})\,^{+7}_{-6}\,(\text{exp.})\,^{+5}_{-4}\,(\text{theory})\text{ fb}$$

$$\sigma_{\text{VBF}} \times B(H \to \gamma\gamma) = 17\,^{+5}_{-4}\text{ fb} = 17\,^{+4}_{-4}\,(\text{stat.})\,^{+2}_{-2}\,(\text{exp.})\,^{+2}_{-2}\,(\text{theory})\text{ fb}$$

$$\sigma_{\text{VH}} \times B(H \to \gamma\gamma) = 3\,^{+4}_{-4}\text{ fb} = 3\,^{+4}_{-3}\,(\text{stat.})\,^{+1}_{-1}\,(\text{exp.})\,^{+1}_{-0}\,(\text{theory})\text{ fb}$$

$$\sigma_{\text{top}} \times B(H \to \gamma\gamma) = 0.7\,^{+0.9}_{-0.7}\text{ fb} = 0.7\,^{+0.8}_{-0.7}\,(\text{stat.})\,^{+0.2}_{-0.1}\,(\text{exp.})\,^{+0.1}_{-0.0}\,(\text{theory})\text{ fb}$$

Standard Model expectations

$$\sigma_{\text{ggH}} \times B(H \to \gamma\gamma) = 102\,^{+19}_{-18}\text{ fb} = 102^{+17}_{-17}\,(\text{stat.})\,^{+8}_{-6}\,(\text{exp.})\,^{+4}_{-3}\,(\text{theory})\text{ fb}$$

$$\sigma_{\text{VBF}} \times B(H \to \gamma\gamma) = 8\,^{+4}_{-3}\text{ fb} = 8\,^{+3}_{-3}\,(\text{stat.})\,^{+1}_{-1}\,(\text{exp.})\,^{+1}_{-1}\,(\text{theory})\text{ fb}$$

$$\sigma_{\text{VH}} \times B(H \to \gamma\gamma) = 5\,^{+4}_{-3}\text{ fb} = 5\,^{+4}_{-3}\,(\text{stat.})\,^{+1}_{-1}\,(\text{exp.})\,^{+0}_{-0}\,(\text{theory})\text{ fb}$$

$$\sigma_{\text{top}} \times B(H \to \gamma\gamma) = 1.3\,^{+0.9}_{-0.8}\text{ fb} = 1.3\,^{+0.9}_{-0.8}\,(\text{stat.})\,^{+0.2}_{-0.1}\,(\text{exp.})\,^{+0.2}_{-0.1}\,(\text{theory})\text{ fb}$$

Expected and observed local significances of the VBF, VH and top-quark associated production modes

Measurement	Exp. Z_0	Obs. Z_0
μ_{VBF}	$2.6\,\sigma$	$4.9\,\sigma$
μ_{VH}	$1.4\,\sigma$	$0.8\,\sigma$
μ_{top}	$1.8\,\sigma$	$1.0\,\sigma$

H→γγ

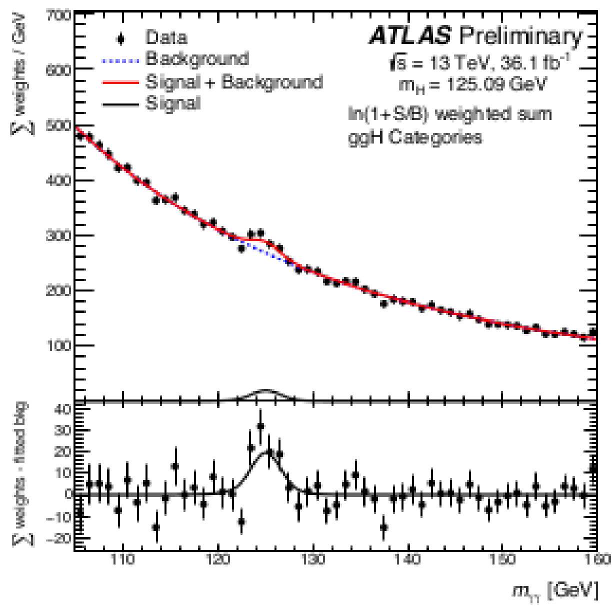
ATLAS Preliminary
√s = 13 TeV, 36.1 fb-1
mH = 125.09 GeV
ln(1+S/B) weighted sum
ggH Categories
Data
Background
Signal + Background
Signal
∑ weights / GeV
∑ weights - fitted bkg
mγγ [GeV]

(a)

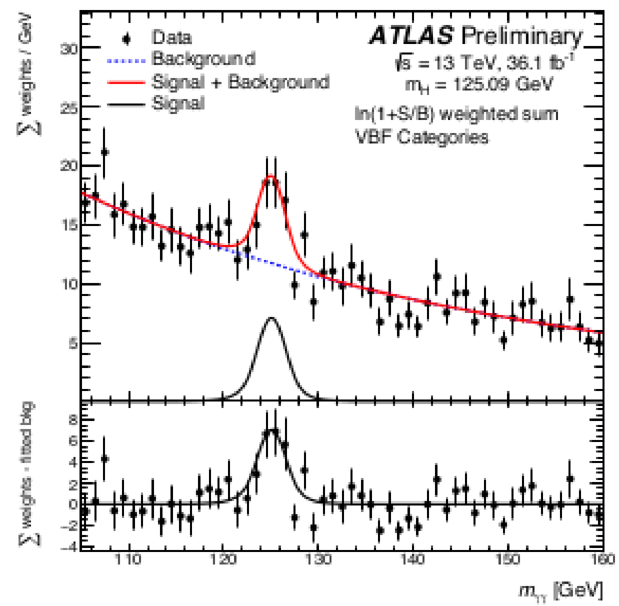
ATLAS Preliminary
√s = 13 TeV, 36.1 fb-1
mH = 125.09 GeV
ln(1+S/B) weighted sum
VBF Categories
Data
Background
Signal + Background
Signal
∑ weights / GeV
∑ weights - fitted bkg
mγγ [GeV]

(b)

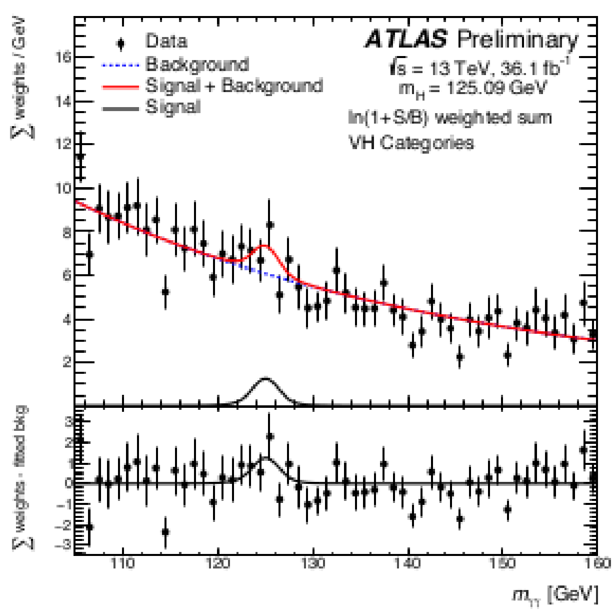
ATLAS Preliminary
√s = 13 TeV, 36.1 fb-1
mH = 125.09 GeV
ln(1+S/B) weighted sum
VH Categories
Data
Background
Signal + Background
Signal
∑ weights / GeV
∑ weights - fitted bkg
mγγ [GeV]

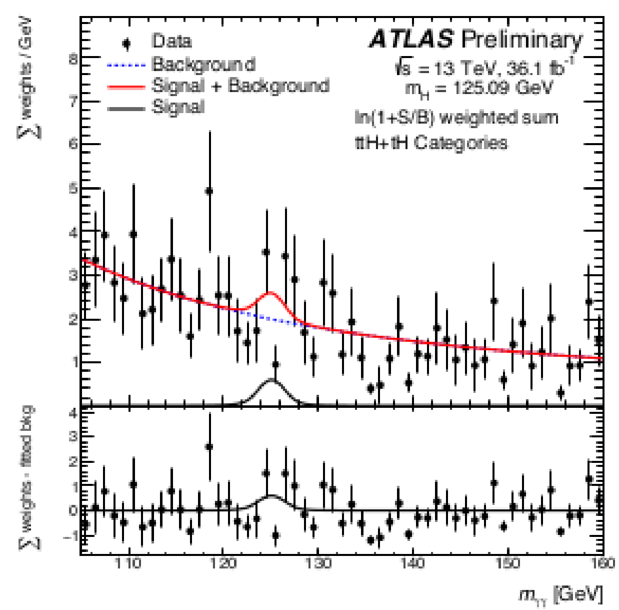
ATLAS Preliminary
√s = 13 TeV, 36.1 fb-1
mH = 125.09 GeV
ln(1+S/B) weighted sum
ttH+tH Categories
Data
Background
Signal + Background
Signal
∑ weights / GeV
∑ weights - fitted bkg
mγγ [GeV]

H→γγ

Selections used for the fiducial space definition

Objects	Definition
Photons	$\lvert\eta\rvert < 1.37$ OR $1.52 < \lvert\eta\rvert < 2.37$, $p_T^{\text{iso},0.2}/p_T^{\gamma} < 0.05$
Jets	anti-k_t, $R = 0.4$, $p_T > 30\,\text{GeV}$, $\lvert y\rvert < 4.4$
Leptons, ℓ	e or μ, $p_T > 15\,\text{GeV}$, $\lvert\eta\rvert < 2.47$ (excluding $1.37 < \lvert\eta\rvert < 1.52$ for $\ell = e$)

Fiducial region	Definition
Diphoton fiducial	$N_\gamma \geq 2$, $p_T^{\gamma_1} > 0.35\,m_{\gamma\gamma}$, $p_T^{\gamma_2} > 0.25\,m_{\gamma\gamma}$
VBF-enhanced	Diphoton fiducial, $N_j \geq 2$, $m_{jj} > 400$ GeV, $\lvert\Delta y_{jj}\rvert > 2.8$, $\lvert\Delta\phi_{\gamma\gamma,jj}\rvert > 2.6$
$N_{\text{lepton}} \geq 1$	Diphoton fiducial, $N_\ell \geq 1$
High E_T^{miss}	Diphoton fiducial, $E_T^{\text{miss}} > 80$ GeV, $p_T^{\gamma\gamma} > 80$ GeV
$t\bar{t}H$-enhanced	Diphoton fiducial, $\left(N_j \geq 4,\ N_{\text{b-jets}} \geq 1\right)$ OR $\left(N_j \geq 3,\ N_{\text{b-jets}} \geq 1, N_\ell \geq 1\right)$

H→γγ, Classification of the Higgs boson production modes (STXS)

Process	Measurement region	Stage 1 region
ggH + $gg \to Z(\to qq)H$	0-jet	0-jet
	1-jet, $p_T^H < 60$ GeV	1-jet, $p_T^H < 60$ GeV
	1-jet, $60 \leq p_T^H < 120$ GeV	1-jet, $60 \leq p_T^H < 120$ GeV
	1-jet, $120 \leq p_T^H < 200$ GeV	1-jet, $120 \leq p_T^H < 200$ GeV
	$\geq$ 1-jet, $p_T^H > 200$ GeV	1-jet, $p_T^H > 200$ GeV
		$\geq$ 2-jet, $p_T^H > 200$ GeV
	$\geq$ 2-jet, $p_T^H < 200$ GeV or VBF-like	$\geq$ 2-jet, $p_T^H < 60$ GeV
		$\geq$ 2-jet, $60 \leq p_T^H < 120$ GeV
		$\geq$ 2-jet, $120 \leq p_T^H < 200$ GeV
		VBF-like, $p_T^{Hjj} < 25$ GeV
		VBF-like, $p_T^{Hjj} \geq 25$ GeV
$qq' \to Hqq'$ (VBF + VH)	$p_T^j < 200$ GeV	$p_T^j < 200$ GeV, VBF-like, $p_T^{Hjj} < 25$ GeV
		$p_T^j < 200$ GeV, VBF-like, $p_T^{Hjj} \geq 25$ GeV
		$p_T^j < 200$ GeV, VH-like
		$p_T^j < 200$ GeV, Rest
	$p_T^j > 200$ GeV	$p_T^j > 200$ GeV
VH (leptonic decays)	VH leptonic	$q\bar{q} \to ZH$, $p_T^Z < 150$ GeV
		$q\bar{q} \to ZH$, 150 GeV $< p_T^Z <$ 250 GeV, 0-jet
		$q\bar{q} \to ZH$, 150 GeV $< p_T^Z <$ 250 GeV, $\geq$ 1-jet
		$q\bar{q} \to ZH$, $p_T^Z > 250$ GeV
		$q\bar{q} \to WH$, $p_T^W < 150$ GeV
		$q\bar{q} \to WH$, 150 GeV $< p_T^W <$ 250 GeV, 0-jet
		$q\bar{q} \to WH$, 150 GeV $< p_T^W <$ 250 GeV, $\geq$ 1-jet
		$q\bar{q} \to WH$, $p_T^W > 250$ GeV
		$gg \to ZH$, $p_T^Z < 150$ GeV
		$gg \to ZH$, $p_T^Z > 150$ GeV, 0-jet
		$gg \to ZH$, $p_T^Z > 150$ GeV, $\geq$ 1-jet
top-associated production	top	$t\bar{t}H$
		tHW
		$tHqb$
$b\bar{b}H$	merged w/ ggH	$b\bar{b}H$

H→γγ, Classification of the Higgs boson production modes (STXS)

Category	Selection
tH lep 0fwd	$N_{\rm lep}=1, N_{\rm jets}^{\rm cen}\leq 3, N_{\rm b-tag}\geq 1, N_{\rm jets}^{\rm fwd}=0\ (p_{\rm T}^{\rm jet}>25\,{\rm GeV})$
tH lep 1fwd	$N_{\rm lep}=1, N_{\rm jets}^{\rm cen}\leq 4, N_{\rm b-tag}\geq 1, N_{\rm jets}^{\rm fwd}\geq 1\ (p_{\rm T}^{\rm jet}>25\,{\rm GeV})$
ttH lep	$N_{\rm lep}\geq 1, N_{\rm jets}^{\rm cen}\geq 2, N_{\rm b-tag}\geq 1, Z_{\ell\ell}$ veto $(p_{\rm T}^{\rm jet}>25\,{\rm GeV})$
ttH had BDT1	$N_{\rm lep}=0, N_{\rm jets}\geq 3, N_{\rm b-tag}\geq 1, {\rm BDT}_{\rm ttH}>0.92$
ttH had BDT2	$N_{\rm lep}=0, N_{\rm jets}\geq 3, N_{\rm b-tag}\geq 1, 0.83<{\rm BDT}_{\rm ttH}<0.92$
ttH had BDT3	$N_{\rm lep}=0, N_{\rm jets}\geq 3, N_{\rm b-tag}\geq 1, 0.79<{\rm BDT}_{\rm ttH}<0.83$
ttH had BDT4	$N_{\rm lep}=0, N_{\rm jets}\geq 3, N_{\rm b-tag}\geq 1, 0.52<{\rm BDT}_{\rm ttH}<0.79$
tH had 4j1b	$N_{\rm lep}=0, N_{\rm jets}^{\rm cen}=4, N_{\rm b-tag}=1\ (p_{\rm T}^{\rm jet}>25\,{\rm GeV})$
tH had 4j2b	$N_{\rm lep}=0, N_{\rm jets}^{\rm cen}=4, N_{\rm b-tag}\geq 2\ (p_{\rm T}^{\rm jet}>25\,{\rm GeV})$
VH dilep	$N_{\rm lep}\geq 2, 70\,{\rm GeV}\leq m_{\ell\ell}\leq 110\,{\rm GeV}$
VH lep HIGH	$N_{\rm lep}=1, \lvert m_{e\gamma}-89\,{\rm GeV}\rvert>5\,{\rm GeV}, p_{\rm T}^{l+E_{\rm T}^{\rm miss}}>150\,{\rm GeV}$
VH lep LOW	$N_{\rm lep}=1, \lvert m_{e\gamma}-89\,{\rm GeV}\rvert>5\,{\rm GeV}, p_{\rm T}^{l+E_{\rm T}^{\rm miss}}<150\,{\rm GeV}, E_{\rm T}^{\rm miss}$ significance >1
VH MET HIGH	$150\,{\rm GeV}<E_{\rm T}^{\rm miss}<250\,{\rm GeV}, E_{\rm T}^{\rm miss}$ significance >9 or $E_{\rm T}^{\rm miss}>250\,{\rm GeV}$
VH MET LOW	$80\,{\rm GeV}<E_{\rm T}^{\rm miss}<150\,{\rm GeV}, E_{\rm T}^{\rm miss}$ significance >8
jet BSM	$p_{\rm T,j1}>200\,{\rm GeV}$
VH had tight	$60\,{\rm GeV}<m_{\rm jj}<120\,{\rm GeV}, {\rm BDT}_{\rm VH}>0.78$
VH had loose	$60\,{\rm GeV}<m_{\rm jj}<120\,{\rm GeV}, 0.35<{\rm BDT}_{\rm VH}<0.78$
VBF tight, high p_T^{Hjj}	$\Delta\eta_{\rm jj}>2, \lvert\eta_{\gamma\gamma}-0.5(\eta_{\rm j1}+\eta_{\rm j2})\rvert<5, p_T^{Hjj}>25\,{\rm GeV}, {\rm BDT}_{\rm VBF}>0.47$
VBF loose, high p_T^{Hjj}	$\Delta\eta_{\rm jj}>2, \lvert\eta_{\gamma\gamma}-0.5(\eta_{\rm j1}+\eta_{\rm j2})\rvert<5, p_T^{Hjj}>25\,{\rm GeV}, -0.32<{\rm BDT}_{\rm VBF}<0.47$
VBF tight, low p_T^{Hjj}	$\Delta\eta_{\rm jj}>2, \lvert\eta_{\gamma\gamma}-0.5(\eta_{\rm j1}+\eta_{\rm j2})\rvert<5, p_T^{Hjj}<25\,{\rm GeV}, {\rm BDT}_{\rm VBF}>0.87$
VBF loose, low p_T^{Hjj}	$\Delta\eta_{\rm jj}>2, \lvert\eta_{\gamma\gamma}-0.5(\eta_{\rm j1}+\eta_{\rm j2})\rvert<5, p_T^{Hjj}<25\,{\rm GeV}, 0.26<{\rm BDT}_{\rm VBF}<0.87$
ggH 2J BSM	≥ 2 jets, $p_{\rm T}^{\gamma\gamma}\geq 200\,{\rm GeV}$
ggH 2J HIGH	≥ 2 jets, $p_{\rm T}^{\gamma\gamma}\in[120,200]\,{\rm GeV}$
ggH 2J MED	≥ 2 jets, $p_{\rm T}^{\gamma\gamma}\in[60,120]\,{\rm GeV}$
ggH 2J LOW	≥ 2 jets, $p_{\rm T}^{\gamma\gamma}\in[0,60]\,{\rm GeV}$
ggH 1J BSM	$=1$ jet, $p_{\rm T}^{\gamma\gamma}\geq 200\,{\rm GeV}$
ggH 1J HIGH	$=1$ jet, $p_{\rm T}^{\gamma\gamma}\in[120,200]\,{\rm GeV}$
ggH 1J MED	$=1$ jet, $p_{\rm T}^{\gamma\gamma}\in[60,120]\,{\rm GeV}$
ggH 1J LOW	$=1$ jet, $p_{\rm T}^{\gamma\gamma}\in[0,60]\,{\rm GeV}$
ggH 0J FWD	$=0$ jets, one photon with $\lvert\eta\rvert>0.95$
ggH 0J CEN	$=0$ jets, two photons with $\lvert\eta\rvert\leq 0.95$

H→γγ, cross-sections (STXS)

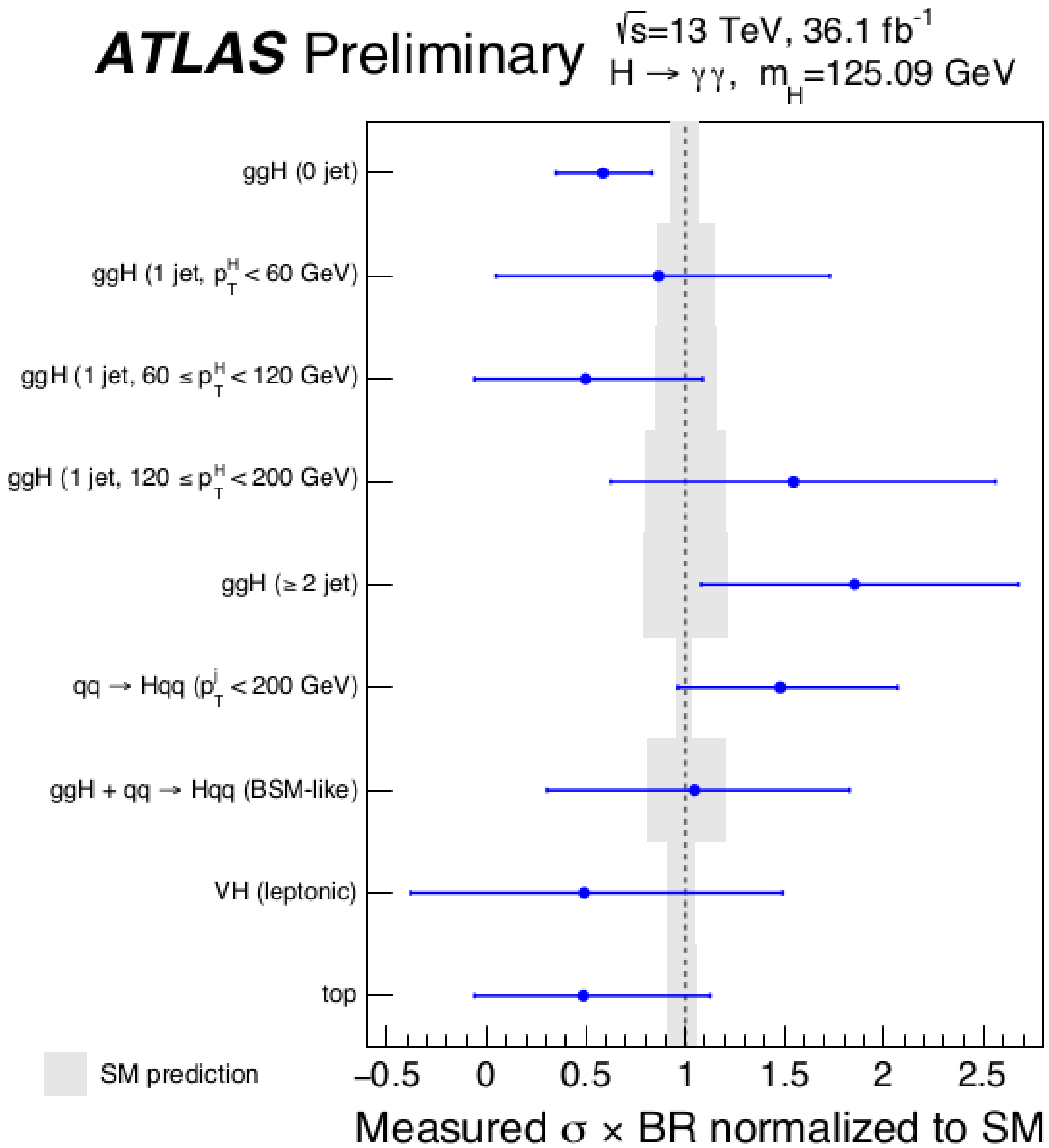

H→γγ - MC generators

Higgs boson production via gluon fusion (ggH) is simulated at next-to-next-to-leading-order (NNLO) accuracy in QCD using the POWHEG NNLOPS [25] program, with the PDF4LHC15 parton distribution function (PDF) set [26]. These sample use the MiNLO approach [27], which achieves next-to-leading-order precision for both the inclusive and the H + 1-jet process in QCD. In addition, POWHEG NNLOPS improves the precision for inclusive observables to NNLO accuracy in QCD by a dedicated reweighting in Higgs boson rapidity using the HNNLO calculation [28]. The Higgs transverse momentum spectrum obtained with this sample was found to be compatible with the results obtained using QCD resummation with next-to-next-to-leading logarithmic (NNLL)+NLO precision from the HRES 2.3 calculation [29, 30]. The HRES prediction includes the effects of the finite top and bottom quark masses up to NLO precision in QCD and use dynamical renormalization (μ_R) and factorization (μ_F) scales, $\mu_F = \mu_R = 0.5\sqrt{m_H^2 + p_{\mathrm{T}}^{H2}}$. The parton-level events produced by the POWHEG NNLOPS program are passed to PYTHIA8 [31] to provide parton showering, hadronization and multiple parton interactions (MPI), using the AZNLO set of parameters that are tuned to data [32]. The sample is normalized such that it reproduces the total cross section predicted by a next-to-next-to-next-to-leading-order ($\mathrm{N^3LO}$) QCD calculation with NLO electroweak corrections applied [33–36].

The measurements are compared to several state-of-the-art predictions of gluon fusion:

- The POWHEG NNLOPS calculation is normalized to the $\mathrm{N^3LO}$ prediction of Refs. [10, 26, 33–36] using a K-factor of $K_{\mathrm{ggH}} = 1.1$. This prediction is labeled as 'default MC' in the plots.
- RADISH+NNLOJET [104] provides $p_{\mathrm{T}}^{\gamma\gamma}$ predictions using a p_{T}^{H} resummation to NNLL and matching to the one jet NNLO differential spectrum from NNLOJET [105]. The shown RADISH+NNLOJET prediction does not include corrections from the finite top and bottom quark masses.
- SCETLIB provides predictions for $|y_{\gamma\gamma}|$, $|\Delta y_{\gamma\gamma}|$, and $|\cos\theta^*|$ at NNLO+NNLL$_\phi$' accuracy[7] derived by applying a resummation of the virtual corrections to the gluon form factor [106, 107]. The underlying NNLO predictions are obtained using MCFM8 with zero-jettiness subtractions [108, 109].

H→ZZ*→4ℓ and H→γγ combination

- Leading uncertainties on the global signal strength

$$\mu = 1.09 \pm 0.12 = 1.09 \pm 0.09\,(\text{stat.})\ ^{+0.06}_{-0.05}\,(\text{exp.})\ ^{+0.06}_{-0.05}\,(\text{th.})$$

Source	Up	Down
Theoretical		
$\sigma_{\text{ggF}}^{\text{SM}}$ (perturbative)	−0.045	+0.044
PDFs	±0.018	
Branching fractions	±0.014	
α_S	−0.011	+0.012
Experimental		
Luminosity	−0.037	+0.038
Energy resolution (e, γ)	+0.021	−0.019
Pileup	+0.014	−0.015

H→WW* (summary from Run 1)

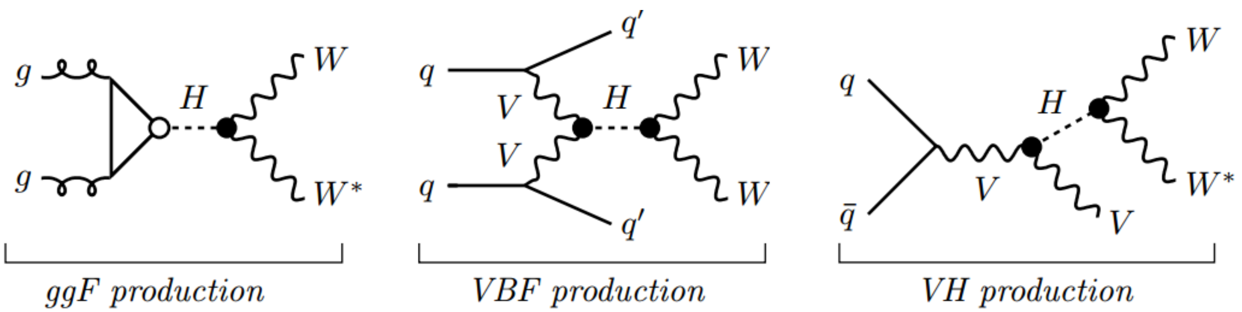

- Dataset: ~25 fb^{-1} @ 7-8 TeV

ggF/VBF arXiv:1412.2641v2

WH/ZH arXiv:1506.06641

- 2nd largest Higgs branching fraction → BR(H→WW*) ~ 22%
- Access for measurement of the Higgs boson couplings with vectors bosons (W and Z) and fermions (top mainly)
- Discovery at Run-1 with the full combination among ggF, VBF, WH and ZH modes
  - ggF → observed (expected) significance: 4.3σ (4.3σ)
  - VBF → observed (expected) significance: 3.2σ (2.7σ)
  - WH + ZH → observed (expected) significance: 2.5σ (0.9σ)
  - **Combination → observed (expected) significance: 6.5σ (5.9σ)**

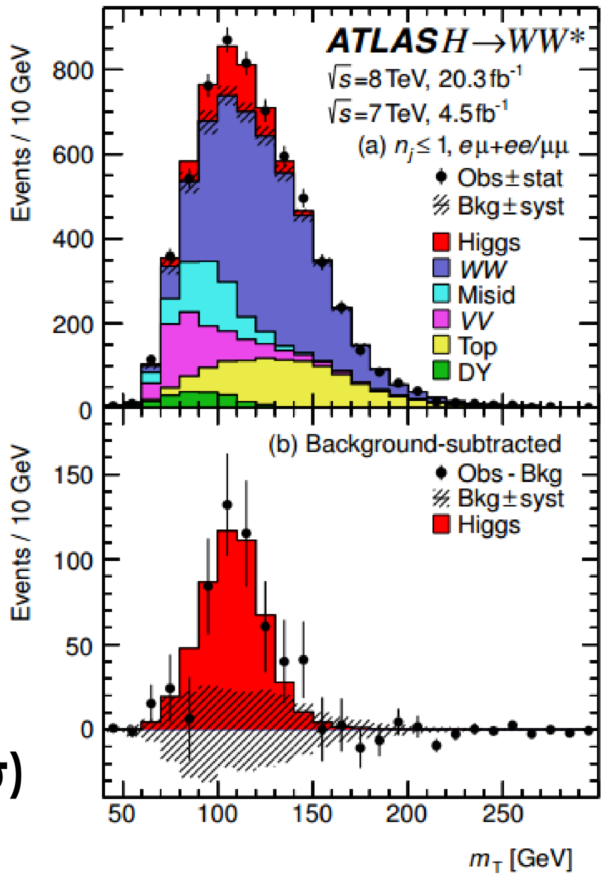

ggF and VBF (H→WW*) results (Run 1)

Sample	Signal significance: Exp. Z_0	Obs. Z_0	Bar graph of observed Z_0	Expected Tot err +	Expected Tot err −	Observed Tot err +	Observed Tot err −	Stat err +	Stat err −	Syst err +	Syst err −	μ_{obs}	μ_{obs} ± stat (thick) ± total (thin)
$n_j = 0$	3.70	4.08		0.35	0.30	0.37	0.32	0.22	0.22	0.30	0.23	1.15	
$e\mu$, $\ell_2 = \mu$	2.89	3.07		0.41	0.36	0.43	0.38	0.30	0.29	0.32	0.24	1.08	
$e\mu$, $\ell_2 = e$	2.36	3.12		0.49	0.44	0.54	0.48	0.38	0.37	0.39	0.30	1.40	
$ee/\mu\mu$ category	1.43	0.71		0.74	0.70	0.68	0.66	0.45	0.44	0.51	0.50	0.47	
$n_j = 1$	2.60	2.49		0.51	0.41	0.50	0.41	0.33	0.32	0.38	0.26	0.96	
$e\mu$ category	2.56	2.83		0.51	0.42	0.56	0.45	0.35	0.35	0.43	0.29	1.16	
$ee/\mu\mu$ category	1.02	0.21		1.12	0.98	1.02	0.97	0.80	0.76	0.63	0.61	0.19	
$n_j \geq 2$, ggF, $e\mu$	1.21	1.44		0.96	0.83	0.91	0.84	0.70	0.68	0.70	0.49	1.20	
$n_j \geq 2$, VBF-enr.	3.38	3.84		0.42	0.36	0.45	0.38	0.36	0.33	0.27	0.19	1.20	
$e\mu$ category	3.01	3.02		0.48	0.40	0.47	0.39	0.40	0.35	0.24	0.16	0.98	
$ee/\mu\mu$ category	1.58	2.96		0.84	0.67	0.97	0.78	0.83	0.71	0.51	0.33	1.98	
All n_j, all signal	5.76	6.06		0.23	0.20	0.23	0.21	0.16	0.15	0.17	0.14	1.09	
ggF as signal	4.34	4.28		0.30	0.24	0.29	0.26	0.19	0.19	0.22	0.18	1.02	
VBF as signal	2.67	3.24		0.50	0.43	0.53	0.45	0.44	0.40	0.30	0.21	1.27	
			0 1 2 3 4 5 6										-1 0 1 2 3

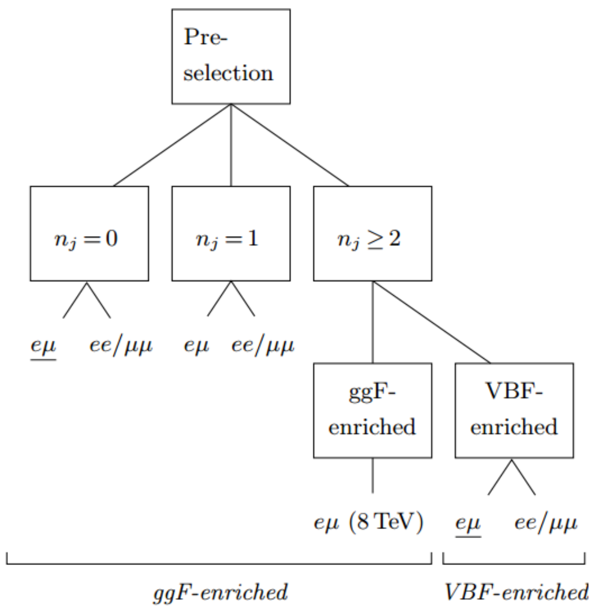

$H \to WW^*$ uncertainties (Run 1)

Source	Observed $\mu = 1.09$ Error +	−	Plot of error (scaled by 100)	Observed $\mu_{ggF} = 1.02$ Error +	−	Plot of error (scaled by 100)	Observed $\mu_{VBF} = 1.27$ Error +	−	Plot of error (scaled by 100)
Data statistics	0.16	0.15		0.19	0.19		0.44	0.40	
Signal regions	0.12	0.12		0.14	0.14		0.38	0.35	
Profiled control regions	0.10	0.10		0.12	0.12		0.21	0.18	
Profiled signal regions	-	-	-	0.03	0.03		0.09	0.08	
MC statistics	0.04	0.04		0.06	0.06		0.05	0.05	
Theoretical systematics	0.15	0.12		0.19	0.16		0.22	0.15	
Signal $H \to WW^*$ $\mathcal{B}$	0.05	0.04		0.05	0.03		0.07	0.04	
Signal ggF cross section	0.09	0.07		0.13	0.09		0.03	0.03	
Signal ggF acceptance	0.05	0.04		0.06	0.05		0.07	0.07	
Signal VBF cross section	0.01	0.01		-	-	-	0.07	0.04	
Signal VBF acceptance	0.02	0.01		-	-	-	0.15	0.08	
Background WW	0.06	0.06		0.08	0.08		0.07	0.07	
Background top quark	0.03	0.03		0.04	0.04		0.06	0.06	
Background misid. factor	0.05	0.05		0.06	0.06		0.02	0.02	
Others	0.02	0.02		0.02	0.02		0.03	0.03	
Experimental systematics	0.07	0.06		0.08	0.08		0.18	0.14	
Background misid. factor	0.03	0.03		0.04	0.04		0.02	0.01	
Bkg. $Z/\gamma^* \to ee, \mu\mu$	0.02	0.02		0.03	0.03		0.01	0.01	
Muons and electrons	0.04	0.04		0.05	0.04		0.03	0.02	
Missing transv. momentum	0.02	0.02		0.02	0.01		0.05	0.05	
Jets	0.03	0.02		0.03	0.03		0.15	0.11	
Others	0.03	0.02		0.03	0.03		0.06	0.06	
Integrated luminosity	0.03	0.03		0.03	0.02		0.05	0.03	
Total	0.23	0.21		0.29	0.26		0.53	0.45	
			-30 -15 0 15 30			-30 -15 0 15 30			-60 -30 0 30 60

H→WW* results: coupling modifiers (Run 1)

ggF + VBF

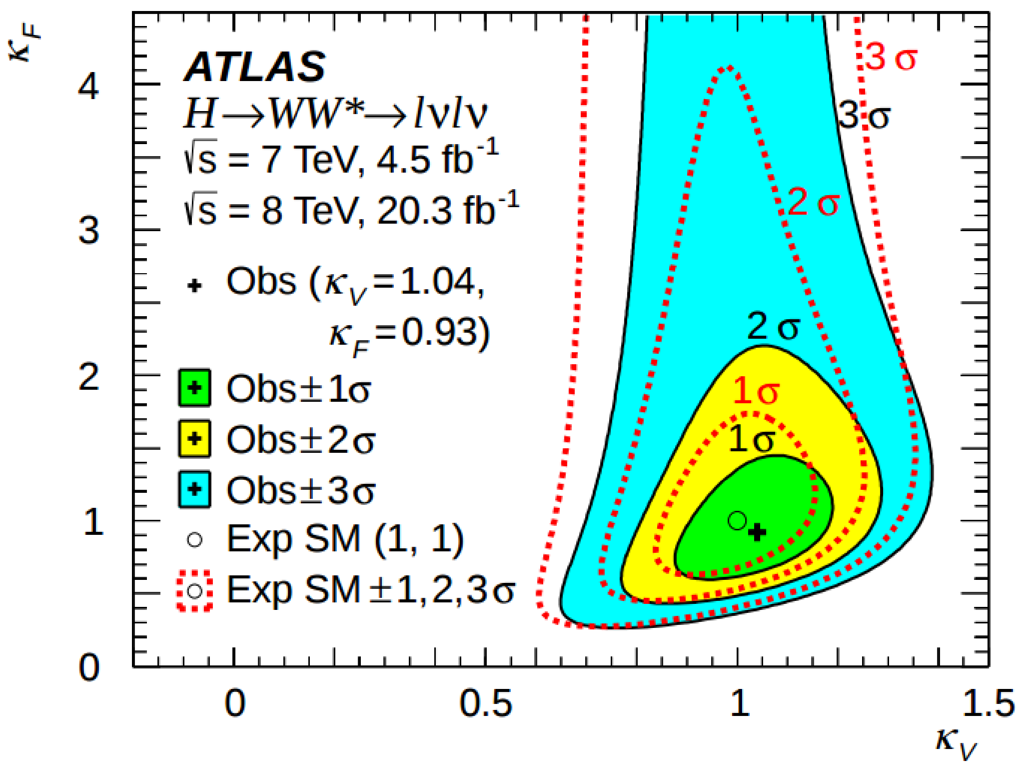

arXiv:1412.2641v2

ggF + VBF + WH + ZH

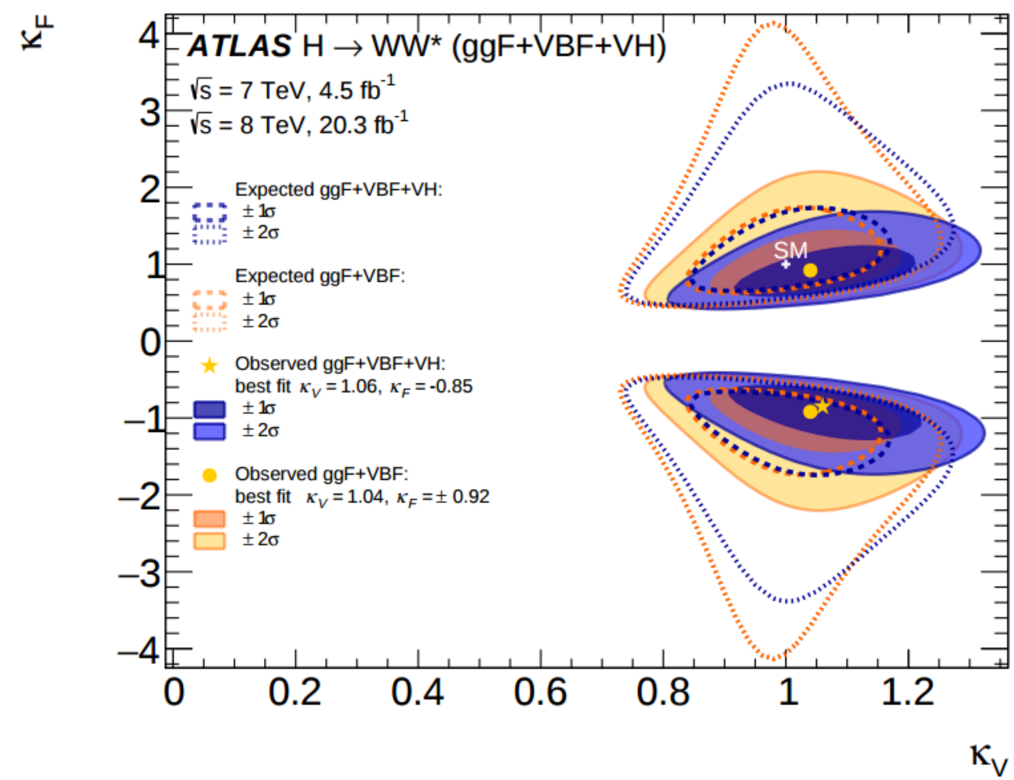

arXiv:1506.06641

H→WW* (Run 2)

VBF

Source	$\Delta\mu_{\mathrm{VBF}}/\mu_{\mathrm{VBF}}$ [%]
Statistical	+60 / -50
Fake factor, sample composition	+18 / -15
MC statistical	±15
VBF generator	+14 / -5
WW generator	+11 / -7
QCD scale for ggF signal for $N_{\mathrm{jet}} \geq 3$	+8 / -7
Jet energy resolution	+8 / -7
b-tagging	+8 / -6
Pile-up	+8 / -6
QCD scale for ggF signal for $N_{\mathrm{jet}} \geq 2$	±6
JES flavour composition	+6 / -4
WW renormalisation scale	±5
Total systematic	+33 / -26
Total uncertainty	+70 / -50

WH

Source	$\Delta\mu_{WH}/\mu_{WH}$ [%]
Statistical	+120 / -100
MC statistical	+60 / -70
Pile-up	+22 / -26
Jet energy resolution	+22 / -23
Top-quark generator	+17 / -20
b-tagging	+10 / -11
Top-quark PS/UE	+7 / -8
JES flavour comp.	+8 / -5
JES η intercalibration	+7 / -6
$WZ/W\gamma^*$ generator	+7 / -6
Top-quark QCD scales	+6 / -7
$WZ/W\gamma^*$ resum. scale	±5
Total systematic	+70 / -80
Total uncertainty	+140 / -130

$$\sigma_{\mathrm{VBF}} \cdot \mathcal{B}_{H\to WW^*} = 1.4^{+0.8}_{-0.6}(\mathrm{stat})^{+0.5}_{-0.4}(\mathrm{sys})\ \mathrm{pb}$$

SM prediction: 0.808 ± 0.021 pb

$$\sigma_{WH} \cdot \mathcal{B}_{H\to WW^*} = 0.9^{+1.1}_{-0.9}(\mathrm{stat})^{+0.7}_{-0.8}(\mathrm{sys})\ \mathrm{pb}$$

SM prediction: 0.293 ± 0.007 pb

Higgs width

$$\mu_{\text{off-shell}}(\hat{s}) \equiv \frac{\sigma^{gg\to H^*\to VV}_{\text{off-shell}}(\hat{s})}{\sigma^{gg\to H^*\to VV}_{\text{off-shell, SM}}(\hat{s})} = \kappa^2_{g,\text{off-shell}}(\hat{s}) \cdot \kappa^2_{V,\text{off-shell}}(\hat{s})$$

$$\mu_{\text{on-shell}} \equiv \frac{\sigma^{gg\to H\to VV}_{\text{on-shell}}}{\sigma^{gg\to H\to VV}_{\text{on-shell, SM}}} = \frac{\kappa^2_{g,\text{on-shell}} \cdot \kappa^2_{V,\text{on-shell}}}{\Gamma_H / \Gamma_H^{\text{SM}}}$$

Higgs spin-parity